Laboratory Investigation (2019) 99:1661–1688
https://doi.org/10.1038/s41374-019-0290-1

ARTICLE

TERT assists GDF11 to rejuvenate senescent VEGFR2$^+$/CD133$^+$ cells in elderly patients with myocardial infarction

Lan Zhao[1,2] · Shaoheng Zhang[1,3] · Jin Cui[1] · Weiguang Huang[1] · Jiahong Wang[3] · Feng Su[3] · Nannan Chen[3] · Qunlin Gong[3]

Received: 16 June 2018 / Revised: 31 May 2019 / Accepted: 11 June 2019 / Published online: 10 July 2019

Abstract

Growth differentiation factor 11 (GDF11) is a transforming growth factor β superfamily member with a controversial role in rejuvenating old stem cells after acute injury in the elderly population. This study aimed to evaluate the effects of telomerase reverse transcriptase (TERT) on GDF11-mediated rejuvenation of senescent late-outgrowth endothelial progenitor cells (EPCs), defined as VEGFR2$^+$/CD133$^+$ cells, in elderly patients with acute myocardial infarction (AMI). We compared the quantity and capabilities of VEGFR2$^+$/CD133$^+$ cells from old (>60 years), middle-aged (45–60 years), and young (<45 years) AMI patients. The decline in circulating count and survival of VEGFR2$^+$/CD133$^+$ cells with age was accompanied by decrease in their TERT and GDF11 expression levels in patients with AMI. Further, upregulation of TERT could trigger GDF11-mediated rejuvenation of old VEGFR2$^+$/CD133$^+$ cells by renewing their survival and angiogenic abilities through activation of canonical (Smad2/3) and noncanonical (eNOS) signaling pathways. Depletion of GDF11 or TERT caused senescence of young VEGFR2$^+$/CD133$^+$ cells leading to impaired vascular function and angiogenesis in vitro and in vivo, whereas adTERT and rhGDF11 rescued this senescence. TERT cooperates with GDF11 to enhance regenerative capabilities of old VEGFR2$^+$/CD133$^+$ cells. When combined with TERT, GDF11 may represent a potential therapeutic target for the treatment of elderly patients with MI.

Introduction

Aging is a major risk factor for the occurrence of acute and chronic cardiovascular disease (CVD), including myocardial infarction (MI) [1]. Endothelial dysfunction and injury are known to contribute to the pathogenesis of MI and ischemic heart failure [2]. Endothelial progenitor cells (EPCs) have been evaluated as predictors of CVD outcomes [3], as their number and functionality may reflect the endogenous vascular repair capacity.

Growth differentiation factor 11 (GDF11), a newly discovered member of the bone morphogenetic protein/transforming growth factor β (BMP/TGFβ) superfamily, may play a role in rejuvenating senescent cells. A decrease in GDF11 may be involved in the cellular senescence observed in chronic obstructive pulmonary disease [4]. Circulating GDF11 increases proliferation of brain capillary endothelial cells (ECs) migration of ECs, and improves vascular and neurogenic rejuvenation of the aging mouse brain [5]. However, reports of the effects of GDF11 on human tissues are inconsistent, with some studies describing anti-aging and pro-regenerative activities on the heart and skeletal muscle, while others show the opposite results or no effect [6]. Walker et al. questioned the beneficial effects of recombinant GDF11 (rGDF11) on muscle aging, reporting that supplementation of rGDF11 had no effect in

These authors contributed equally: Lan Zhao, Shaoheng Zhang

Supplementary information The online version of this article (https://doi.org/10.1038/s41374-019-0290-1) contains supplementary material, which is available to authorized users.

✉ Shaoheng Zhang
shaohengzh67@163.com

1 Department of Cardiology, Guangzhou Red Cross Hospital, Medical College of Ji-Nan University, 396 Tongfuzhong Road, Haizhu District, 510220 Guangzhou, China

2 Department of Cardiology, Dahua Hospital, 901 Laohumin Road, Xuhui District, 200237 Shanghai, China

3 Department of Cardiology, Yangpu Hospital, Tongji University School of Medicine, 450 Tengyue Road, 200090 Shanghai, PR China

aged mice and impaired muscle repair in young mice [7]. No mechanistic studies were performed to explain the disparate results reported in literature. Thus, further experiments are needed to clarify the potential differences in transcriptional output of GDF11 signaling in physiological contexts [7].

The replicative lifespan of various primary human cells can be prolonged by induced expression of the human telomerase reverse transcriptase (TERT) gene. Thus, augmentation of telomerase activity by inducing TERT expression is a potential strategy for therapeutic interventions in age-related diseases including MI [8]. The delivery of TERT and other genes into mesenchymal stromal cells (MSCs) may have therapeutic applications for restoring or rejuvenating aged MSCs by increasing vascular endothelial growth factor (VEGF) [9]. We aimed to determine whether TERT facilitates GDF11-mediated rejuvenation of old EPCs by regulating its transcription. We evaluated the effect of add-mediated TERT gene transfer (adTERT) and exogenous recombinant human GDF11 (rhGDF11) on rejuvenation in old EPCs characterized by declined survival and capacity. adTERT activated rhGDF11-mediated canonical (Smad2/3) and noncanonical (eNOS) signaling pathways, and consequently improved survival and angiogenesis of old EPCs. To confirm this potential mechanism, we depleted GDF11 or TERT with the GDF11 antagonist follistatin or GDF11/TERT knockdown in young EPCs derived from a cohort of patients with AMI. We found that depletion of GDF11 or TERT inactivated Smad2/3 and eNOS signals and led to significant decreases in survival and vascular function of young EPCs. We then performed animal studies to demonstrate that depletion of GDF11 or TERT caused senescence and impaired vascular function and angiogenesis in young EPCs engrafted into old MI rat hearts.

Materials and methods

Materials and methods are available in the online-only Data Supplement.

Patients

As shown in Fig. S1, EPCs were derived from primary cell cultures obtained from circulating blood from three age groups with AMI referred within 24 h after symptomatic onset for primary percutaneous coronary intervention (PCI): young, <45 years; middle-aged, 45–60 years old; old, >60 years.

Informed consent was obtained from patients prior to PCI. The study was approved by the Ethics Committees of the Yangpu Hospital and the Guangzhou Red Cross Hospital on the Use of Human Subjects in Research.

Analysis of EPC content in CB-MNCs

Immediately after PCI, 40 mL of circulating blood (CB) was collected from the affected coronary artery of all patients. CB-mononuclear cells (CB-MNCs) were isolated from the samples by using erythrocyte lysis buffer (BD Pharmingen, San Jose, CA, USA) according to the manufacturer's instructions. As shown in Fig. S2, CB-MNCs were randomly divided into two parts: one part was used for quantification of EPCs content; the other was cultured for EPCs. To analyze the EPCs content in the CB-MNCs, fluorescence-activated cell sorting (FACS) analysis was performed to determine their lineage (i.e., $CD133^{+}VEGFR2^{+}$ cell content).

Isolation, culture, identification, and labeling of EPCs

CB-MNCs were plated at a density of $0.8–1.0 \times 10^{6}$ cells/cm^{2} on fibronectin-coated Petri dishes (Sigma-Aldrich) with endothelial cell basal medium (EBM-2). Non-adherent cells were removed on day 4, and cultures were then supplemented with new aliquots of media. After 7–10 days, monolayers of cobblestone-appearing cells were formed. We cultured the cells for a further 21–28 day period and used the late-outgrowth EPCs for subsequent functional tests, molecular assay, and therapy [10]. As shown in Fig. S2, ten patient EPCs cultured from the pooled peripheral blood of the patients of the same age-based group were randomly assigned to experiments on senescence and expression of TERT and GDF11-mediated signaling. A further ten old EPCs received rhGDF11, siGDF11, adTERT, siTERT, SB431542, or L-NAME (an eNOS inhibitor), for experiments on rejuvenation, survival, and neovascularization, and analysis of GDF11-mediated signaling; ten young EPCs were treated with siGDF11, follistatin, adTERT, or siTERT to study their effect on senescence, survival, and function of young EPCs in vitro and the in vivo. Two criteria were predominantly used to identify EPCs, as we described previously [11]: (1) cell surface markers that indicate both cellular naïveté and endothelial origin and (2) functional phenotypes that imply the presence of endothelial precursors.

Prior to cell transplantation, EPCs were collected and transfected with a lentiviral vector containing enhanced green fluorescent protein (EGFP) cDNA, as we described previously [11]. Cells were suspended in ice-cold phosphate-buffered saline (PBS) at a density of 1×10^{7} cells/mL.

Real-time quantitative PCR (qRT-PCR) and immunoblotting

Cultured EPCs and peri-infarct myocardial tissues from the rat tissues were harvested and pulverized to extract RNA or protein for qRT-PCR and immunoblotting, as described in Online Supplemental Data.

Telomerase activity

Telomerase activity was determined using a commercial kit (Telo TAGGG Telomerase PCR ELISA, Roche Applied Science, Indianapolis, IN) as per manufacturer's instructions.

Senescence-associated β-galactosidase activity assay

Senescence-associated β-galactosidase (SA-β-gal) activity was measured using a β-galactosidase staining kit (BioVision, Palo Alto, CA, USA) according to the manufacturer's instructions.

Overexpression or depletion of GDF11 and TERT

rhGDF11 was obtained from PeproTech. The GDF11 antagonist follistatin was obtained through the National Hormone & Pituitary Program and A.F. Parlow, Harbor-UCLA Medical Center (Torrance, CA). Retroviral plasmid vectors (pMXs) encoding TERT expression (Addgene) were transfected with the viral packaging genes gag-pol into EPCs with the Fugene HD reagent, as per manufacturer's instructions. GDF11 or TERT siRNAs and control siRNA duplexes were transfected together with pRL-TK plasmid vector (Promega) containing the *Renilla reniformis* luciferase gene into EPCs with LipofectAMINE 2000, as described previously [12].

Hypoxic treatment

Cells were removed and exposed to hypoxic (1%) oxygen levels in a water-jacketed CO_2 incubator. The hypoxic condition was maintained throughout all subsequent analyses.

Cell proliferation and apoptosis

The proliferation of EPCs was assessed by fluorescence staining for proliferation marker Ki-67. Apoptotic cell death under hypoxic conditions was evaluated through annexin V/propidium iodide (PI) staining and the TUNEL assay.

Enzyme-linked immunosorbent assay (ELISA)

The cell supernatant was collected. ELISA kits (R&D Systems, Minneapolis, MA, USA) were used to quantify levels of endothelial nitric oxide synthase (eNOS), nitric oxide (NO), NOS activity, GDF11, activin A, myostatin, p16, p21, angiopoietin-1 (Ang-1), basic fibroblast growth factor (bFGF), and VEGF per manufacturer instructions.

Immunocytofluorescence

Cells were incubated with primary antibodies and observed under a fluorescence microscope.

GDF11-regulated signaling antibody assays

The effects on GDF11-relative canonical and noncanonical signaling pathways in young EPCs under hypoxia were studied using young EPCs in the deletion of TERT and GDF11 from three individual experiments. The EPCs were lyzed with 2 × cell lysis buffer (RayBiotech, Norcross, GA, USA) and quantified using a human angiogenesis antibody array (ab197418, Abcam) and a human apoptosis antibody array (ab134001, Abcam) [13].

MI model and treatment

Myocardial infarction was induced in male Sprague Dawley old rats (18 months old) [14], obtained from the Shanghai Animal Administration Center, by ligating the left anterior descending coronary artery. The animals were then randomized to receive saline (PBS) injection or cell therapy.

Echocardiography

Cardiac functions were evaluated by echocardiography.

Histology and immunofluorescence

The left ventricles of the remaining rats were weighed to calculate the ratio of left-ventricular weight to body weight. The size of the infarct was obtained by calculating the percentage of the infarcted area against the whole LV area by using a digital imaging program (Scion Image J). The tissues from the autopsy specimens were embedded in paraffin and were then used in immunohistochemistry assays. For immunocytofluorescence, cells were fixed with fresh 4% paraformaldehyde in PBS.

Online Data Supplement tables and figures

Table S1 in the online-only Data Supplement describes the primers for qRT-PCR. Figure S1 in the online-only Data Supplement shows the experimental flow of Study design. Figure S2 in the online-only Data Supplement shows EPC isolation, culture, identification, intervention, and application allocation. Figure S3 in the online-only Data

Supplement shows cell characterization assessed by FACS. Figure S4 in the online-only Data Supplement shows the protein expression of the TGF-β superfamily, GDF11, activin, and myostatin in old $VEGFR2^+/CD133^+$ cells receiving adTERT. Figure S5 in the online-only Data Supplement shows the protein expression of GDF11 in young $VEGFR2^+/CD133^+$ cells receiving follistatin or siGDF11. Figure S6 in the online-only Data Supplement shows overall translation changes in GDF11-regulated signaling antibody assays resulting GDF11 or TERT depletion.

Results

Baseline clinical, angiographic, and procedural characteristics

We chose 118 patients from three age groups (young, <45 years; middle-aged, 45–60 years old; old, >60 years) to examine the effects of aging on EPCs. After matching for sex, body weight, and cardiovascular risk factors, there was no difference in clinical presentation, left-ventricular function, and statistically significant difference in the prevalence of concomitant diseases or history of CVD between three groups. The number of ST elevation myocardial infarction (STEMI) and the characteristics of infarct-related arteries were not different between three groups (Table 1). In addition, no significant difference was seen between the three groups in the incidence of angiographic adverse events (such as contrast induced nephropathy, allergic reactions, and vagal responses), complications related to PCI (side branch closure, abrupt closure, decreased flow during the procedure, angiographic distal embolization, perforation or tamponade, among others), and in the rates of repeated PCI (data not shown). Therefore, we could initially rule out the impact of these cardiovascular disease comorbidities and health habits on EPC function in this model of age-induced impairment of EPC function.

Aging decreases the quantity and function of circulating EPCs in elderly patients

There is more than one endothelial progeny, monocytic veresus hemangioblastic, within the circulating blood, and two distinct cell types of EPCs are currently recognized according to their growth characteristics and morphological appearance: early outgrowth EPCs and late-outgrowth EPCs [15]. EPCs are generally identified as $CD133^+/VEGFR^+$ cells [16, 17]. Previous studies show the migratory activity of circulating EPCs may aid the assessment of secondary risk in AMI patients, and that age-related endothelial dysfunction is accompanied by quantitative and qualitative alterations of the EPCs pool [18]. Likewise, we found an obvious decrease in the number of circulating $CD133^+/VEGFR2^+$ cells in old and middle-aged patients compared with young patients (Fig. 1a, b). The number of circulating blood $CD133^+/VEGFR2^+$ cells negatively correlated with age ($r = -0.821$, $p < 0.001$). To further investigate the senescence of EPCs in old patients, we measured the number and function of EPCs from the three age groups at the time of their emergence in culture. EPCs were identified by both cell surface markers and functional phenotypes. CD146, CD11, and CXCR4 staining were used in flow cytometry to identify early peripheral blood-derived EPCs, in addition to conventional endothelial markers such as CD34, VEGFR2, and CD133 as described by de la Puente et al. [19] and our previous study [11]. We performed FACS to compare the differences between these cell populations in the three groups by using these molecular markers. All EPCs from the three age groups positively expressed CD34, CD146, CD11, CXCR4, VEGFR2, and CD133, and showed a relatively homogeneous cell population. However, the levels of EPCs expressing these markers were significantly lower in the old group than in the young and middle-aged groups ($p < 0.001$ for all comparisons; Fig. 1c). These in vitro findings were in correlation with the decreased CD133/VEGFR2 cell count observed in the circulating blood. We found a significantly smaller proportion of viable cultured EPCs obtained from old patients ($80.81 \pm 1.1\%$) than from young and middle-aged patients ($90.8 \pm 1.1\%$ and $85.0 \pm 0.7\%$, respectively, $p < 0.001$, for all comparisons, Fig. 1d). Cell surface marker examination demonstrated that these cells after 21–28 days of culture were $CD34^+/CD133^+/CD31^+/VEGFR2^+/CD14^-/CD45^-$, characteristic of late-out EPCs [16, 20]. These late-outgrowth EPCs were reduced in the old patients compared with those young (Fig. S3). A functional definition was used in the late-outgrowth EPCs, which formed in vitro colonies with a typical cobblestone morphology, and exhibited migration, and tube formation [21, 22]. The migration activity was significantly lower in the old EPCs compared with the young and middle-aged EPCs (Fig. 1e). The colony formation ability of the EPCs was lowest in the old group (Fig. 1f, i). The number of cobblestone-shaped cells was lower in the old group than in the young and middle-aged groups (Fig. 1h). EPCs from old patients showed a significant impairment of tube-forming ability compared with those from young- and middle-aged patients (Fig. 1g, j). Mature EPCs are terminally differentiated into endothelial cells (ECs) with an angiogenic capability and strong expression of vWF (factor VIII), VEGFR2, CD31, CD146, etc. [21, 22]. Thus, the expression levels of factor VIII were evaluated to determine the vasculogenic capacity of mature EPCs from the three age

Table 1 Summary of patient characteristics (means ± SD, $n = 118$, each group)

Characteristic	Young-aged	Middle-aged	Old-aged	*P*-value
N	37	41	40	
Age (years)	38.8 ± 5.2	54.9 ± 4.0	73.7 ± 6.5	<0.001
Male gender (%)	19 (51.4)	22 (53.7)	20 (50.0)	0.893
Body weight (kg)	68.7 ± 7.2	71.5 ± 6.4	69.2 ± 6.8	0.149
Smoking current (%)	19 (51.3)	23 (56.1)	21 (52.5)	0.827
Pack-years of smoking	5.7 ± 1.0	6.0 ± 0.8	5.8 ± 0.9	0.332
Diabetes (%)	13 (35.1)	18 (43.9)	18 (39.0)	0.600
Fasting glucose (mmol/L)	6.4 ± 1.6	6.8 ± 1.9	6 .5 ± 1.7	0.525
Hypertension (%)	20 (54.1.0)	24 (58.50)	22 (55.0)	0.834
Systolic BP (mm Hg)	146 ± 21	148 ± 19	144 ± 21	0.659
Diastolic BP (mm Hg)	91 ± 17	94 ± 17	92 ± 16	0.765
Hyperlipidemia (%)	26 (70.3)	30 (73.2)	25 (62.5)	0.583
Total cholesterol (mmol/L)	6.4 ± 0.8	6.5 ± 0.7	6.2 ± 0.	0.362
LDL-C (mmol/L)	4.7 ± 0.1	4.6 ± 0.1	4.4 ± 0.1	0.115
HDL-C (mmol/L)	1.22 ± 0.42	1.29 ± 0.55	1.20 ± 0.42	0.736
Triglycerides (mmol/L)	2.9 ± 1.8	3.7 ± 0.4	2.4 ± 2.0	0.067
Chronic renal failure (%)	4 (10.8)	6 (14.6)	7 (17.5)	0.662
Chronic liver disease (%)	5 (13.5)	9 (22.2)	8 (20.0)	0.554
COPD (%)	7 (18.9)	11 (26.8)	12 (30.0)	0.497
Peripheral vascular disease (%)	15 (40.5)	16 (39.0)	21 (52.5)	0.143
Prior myocardial infarction (%)	5 (13.5)	7 (17.1)	9 (22.5)	0.565
Prior stroke (%)	11 (29.7)	14 (34.1)	16 (40.0)	0.629
STEMI (%)	19 (51.4)	22 (53.7)	19 (47.50)	0.861
Killip class >1 (%)	14 (37.8)	20 (48.8)	25 (62.5)	0.214
IRA				
LAD (%)	21 (56.8)	25 (61.0)	26 (65.0)	0.747
LCX (%)	7 (18.9)	10 (24.4)	9 (22.5)	0.764
RCA (%)	9 (24.3)	6 (14.6)	5 (12.5)	0.522

Values are given as no. (%), or means ± SD

BP blood pressure, *HDL-C* high-density lipoprotein cholesterol, *LDL-C* low-density lipoprotein, *COPD* chronic obstructive pulmonary disease, *IRA* infarct-related arteries, *LAD* left anterior descending, *LCX* left circumflex, *RCA* right coronary artery, *MI* myocardial infarction, *Non-STEMI* non-ST elevation myocardial infarction, *STEMI* ST elevation myocardial infarction

groups. As shown in the lower two rows of Fig. 1k, the EPCs from old patients revealed weaker expression of factor VIII in the old group than in the young and middle-aged groups. These data suggest that aging decreases both the quantity and angiogenic function of EPCs from elderly patients with AMI. Because all EPCs used in the following experiments are from late-outgrowth EPCs, these EPCs were defined as the $VEGFR2^+/CD133^+$ cells instead of using the term of "endothelial progenitor cells".

$VEGFR2^+/CD133^+$ cells from elderly patients show increased senescence

Cellular senescence is the limited ability of primary human cells to divide when cultured in vitro [23] and is measured by SA-β-gal activity, senescence markers, p16, and p21 [24]. We first investigated whether aging was associated with cellular senescence of primary cultured human $VEGFR2^+/CD133^+$ cells. Since the molecular definition of EPC self-renewal allows assessment of the quality of presumed EPC preparations [25], we first compared the long culture survival ability of old $VEGFR2^+/CD133^+$ cells with that of young $VEGFR2^+/CD133^+$ cells. To assess the actual role of aging in regulating cellular lifespan, we cultured $VEGFR2^+/CD133^+$ cells from the three age groups under normal conditions until the cells underwent senescence. Long-term culture studies showed that aging significantly shortened the lifespan of $VEGFR2^+/CD133^+$ cells, and influenced cellular lifespan in early and late passages. Aging markedly reduced cell growth in the old $VEGFR2^+/CD133^+$ cells by day 7 (Fig. 2a, b), and accelerated the senescent time of old EPCs (Fig. 2c), suggesting that aging

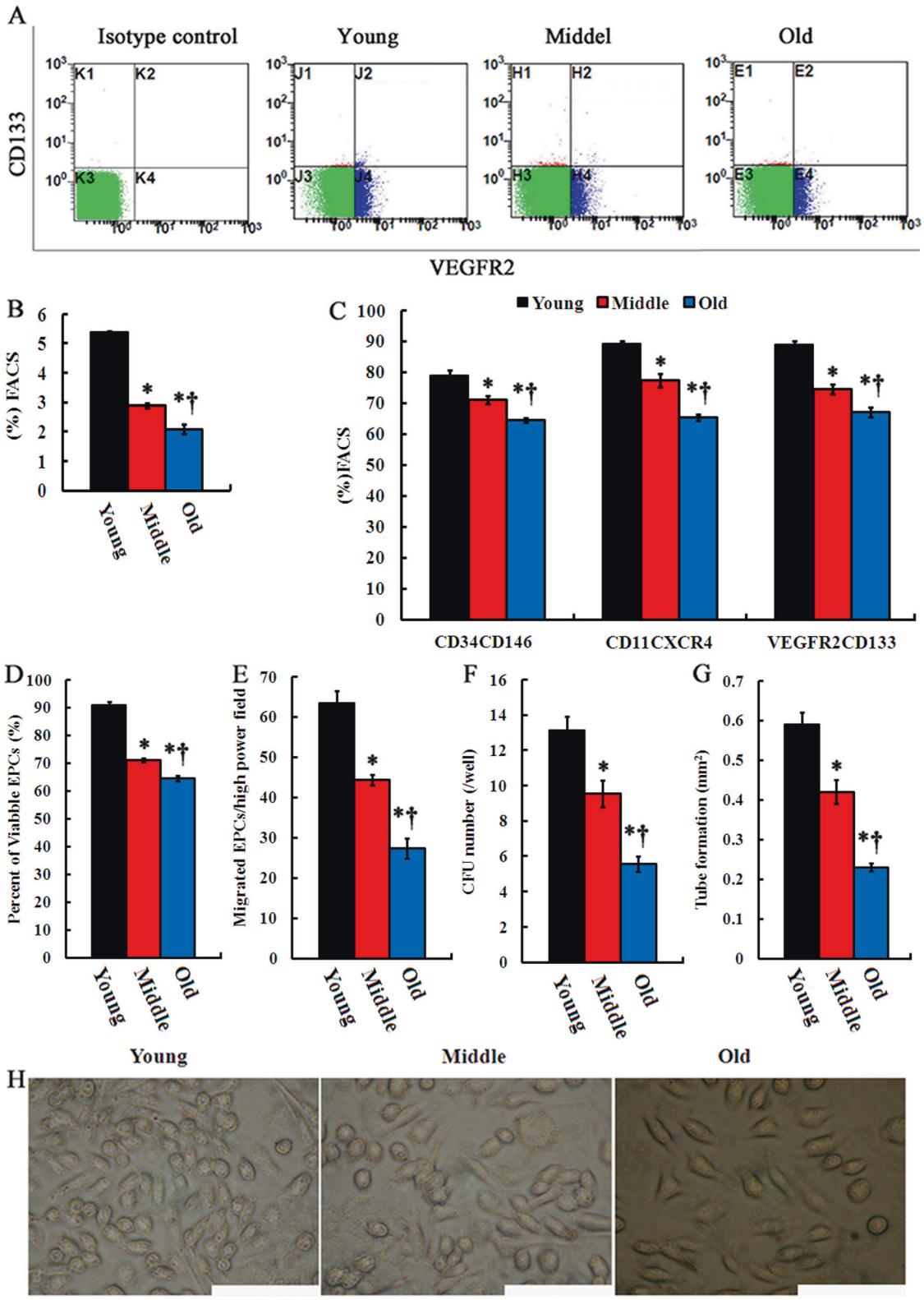

Fig. 1 (Continued)

increased with further cell division and thus promoted senescence. VEGFR2$^+$/CD133$^+$ cells from old, middle-aged, and young patients were stained for SA-β-gal. Old VEGFR2$^+$/CD133$^+$ cells were flattened and enlarged, or appeared like fibroblasts, while young VEGFR2$^+$/CD133$^+$ cells exhibited normal morphology and growth. There was a

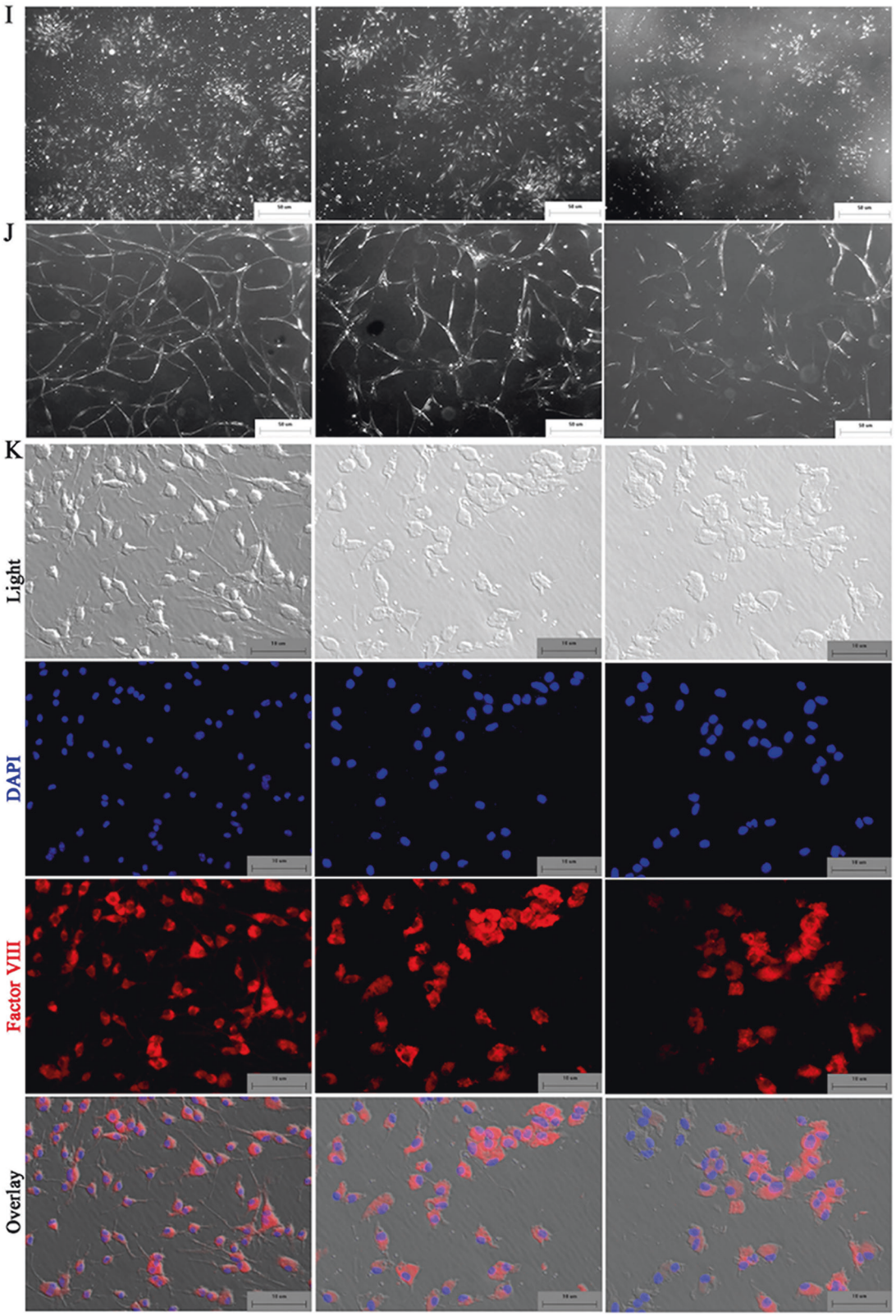

Fig. 1 (Continued)

◀ **Fig. 1** Aging decreased the quantity and function of $CD133^+$/$VEGFR2^+$ cells in circulating blood MNCs. **a** FACS analysis of $CD133^+$/$VEGFR2^+$ cells in circulating MNCs from young, middle-aged, and old patients post-AMI. **b** Quantitative analysis of $CD133^+$/$VEGFR2^+$ cells in circulating MNCs from young, middle-aged, and old patients post-AMI. **c** Percentage of $CD34^+$/$CD146^+$, $CD11^+$/$CXCR4^+$, and $VEGFR2^+$/$CD133^+$ cells in cultured EPCs determined by FACS analysis. **d** Number of viable $CD133^+$/$VEGFR2^+$ cells determined using the MTT proliferation assay. **e** Migratory capacity of $CD133^+$/$VEGFR2^+$ cells. **f** Endothelial colony formation ability (colony formation units, CFU) of $CD133^+$/$VEGFR2^+$ cells. **g** Tube formation ability of $CD133^+$/$VEGFR2^+$ cells. All data are represented as means ± s.e.m. $p < 0.05$: *vs. young group, †vs. middle-aged group ($n = 20$ in each group). (**h**), (**i**), and (**j**) show the typical images of cobblestone growth (**h**), colony formation (**i**), and capillary-like network formation (**j**) of $CD133^+$/$VEGFR2^+$ cells from the various groups, respectively. Scale bars = 50 μm. **k** Representative photomicrograph of $CD133^+$/$VEGFR2^+$ cells characterized by light microscope shape, immunomicroscopy figures of $CD133^+$/$VEGFR2^+$ cells double-stained with labeled with DAPI (4′,6-diamidino-2-phenylindole) and factor VIII. The positive expression of Factor VIII (red) was significantly lower in the old $CD133^+$/$VEGFR2^+$ cells than in the young cells and the middle-aged cells. The nuclei of $CD133^+$/$VEGFR2^+$ cells were stained blue with DAPI. Scale bars = 10 μm

significant increase in the amount of β-galactosidase-positive cells in the old $VEGFR2^+$/$CD133^+$ cells compared with the young $VEGFR2^+$/$CD133^+$ cells (Fig. 2d). Senescence-associated β-galactosidase (SA-β-gal) activity was measured with a β-galactosidase staining kit. $VEGFR2^+$/$CD133^+$ cells from old patients displayed significantly increased SA-β-gal activity compared with young patients (Fig. 2f). These changes of phenotype were suggestive of senescence of old $VEGFR2^+$/$CD133^+$ cells. We also measured p21 and p16 as alternative markers of senescence by immunoblotting and immunofluorescence. Expression of p21 and p16 was increased in $VEGFR2^+$/$CD133^+$ cells from old patients compared with that in those from young patients (Fig. 2e, g–i), confirming that increased senescence observed in $VEGFR2^+$/$CD133^+$ cells from old patients is age-independent.

Expression of TERT and GDF11-mediated signaling in $VEGFR2^+$/$CD133^+$ cells declines with age

Recent studies have shown that treatment with GDF11 significantly inhibited cigarette smoke extract-induced cellular senescence through canonical (Smad2/3) signaling in vitro [4]. eNOS is a target gene of the GDF11-related noncanonical signaling pathway and helps regulate endothelial cell growth and angiogenesis [26]. We measured the differences in telomerase activity and GDF11-related signaling between the three patient groups. qRT-PCR and immunoblotting were performed to evaluate the mRNA and protein expression of GDF11, TERT, and eNOS in $VEGFR2^+$/$CD133^+$ cells. One study reported that circulating GDF11 levels decline with aging and that systemic administration of recombinant GDF11 to aged mice enhances muscle stem cells regenerative capacity after injury [27]. We found mRNA expression and protein levels of GDF11, TERT, and eNOS were the lowest in the $VEGFR2^+$/$CD133^+$ cells from old patients and the highest in those from young patients (Fig. 3a, b). Telomere activity and NOS activity were much lower in the old $VEGFR2^+$/$CD133^+$ cells than in young and middle-aged cells (Fig. 3c, d). Because phosphorylation of eNOS at Ser-1177 is a positive modulator of eNOS activity [28], we measured the eNOS phosphorylation with Ser-1177 antibody. Phosphorylation level of Ser-1177 was the lowest in old $VEGFR2^+$/$CD133^+$ cells (Fig. 3b, e). Similarly, Smad2/3 and their phosphorylation in old EPCs markedly decreased compared with that in $VEGFR2^+$/$CD133^+$ cells from young and middle-aged patients (Fig. 3b, f).

TERT controls GDF11-mediated rejuvenation of older $VEGFR2^+$/$CD133^+$ cells

Our results show that aging could aggravate hypoxia-induced impairment of $VEGFR2^+$/$CD133^+$ cells function involving TERT and GDF11-related signaling in old patients with MI. Next, we determined whether old $VEGFR2^+$/$CD133^+$ cells could benefit from treatment with GDF11 and TERT in vitro. First, we checked whether GDF11 is required for rejuvenation of old $VEGFR2^+$/$CD133^+$ cells by overexpressing and knocking down GDF11. As expected, rhGDF11 treatment resulted in increase in the lifespan of old $VEGFR2^+$/$CD133^+$ cells compared with vehicle treatment under hypoxia, and siGDF11 significantly shortened the lifespan, but addition of rhGDF11 abolished this shortening of siGDF11 (Fig. 4a). We observed a statistically significant increase in population doublings of old $VEGFR2^+$/$CD133^+$ cells with GDF11 treatment (Fig. 4b). These old EPCs treated with rhGDF11 also showed decreased apoptosis and SA-β-gal activity compared with $VEGFR2^+$/$CD133^+$ cells without GDF11 treatment. siGDF11 had the opposite effect (Fig. 4c, d). However, an siGDF11 with a rhGDF11 rescued these effects, showing higher population doublings and lower apoptosis/SA-β-gal activity in siGDF11(+)rhGDF(+) treatment when compared with siGDF11 treatment (Fig. 4b–d). Overall, it appears that GDF11 repletion could rejuvenate old $VEGFR2^+$/$CD133^+$ cells, enhancing their resistance to hypoxia-induced damage, which is consistent with prior reports [29, 30]. Next, we tested if TERT activation is necessary for GDF11 to rejuvenate older $VEGFR2^+$/$CD133^+$ cells under hypoxic conditions. This result is especially of interest since it was previously reported that the TGF-β superfamily, specifically myostatin, GDF11, and activin, is associated with aging with varying degrees of potency [27]. In order to confirm that TERT

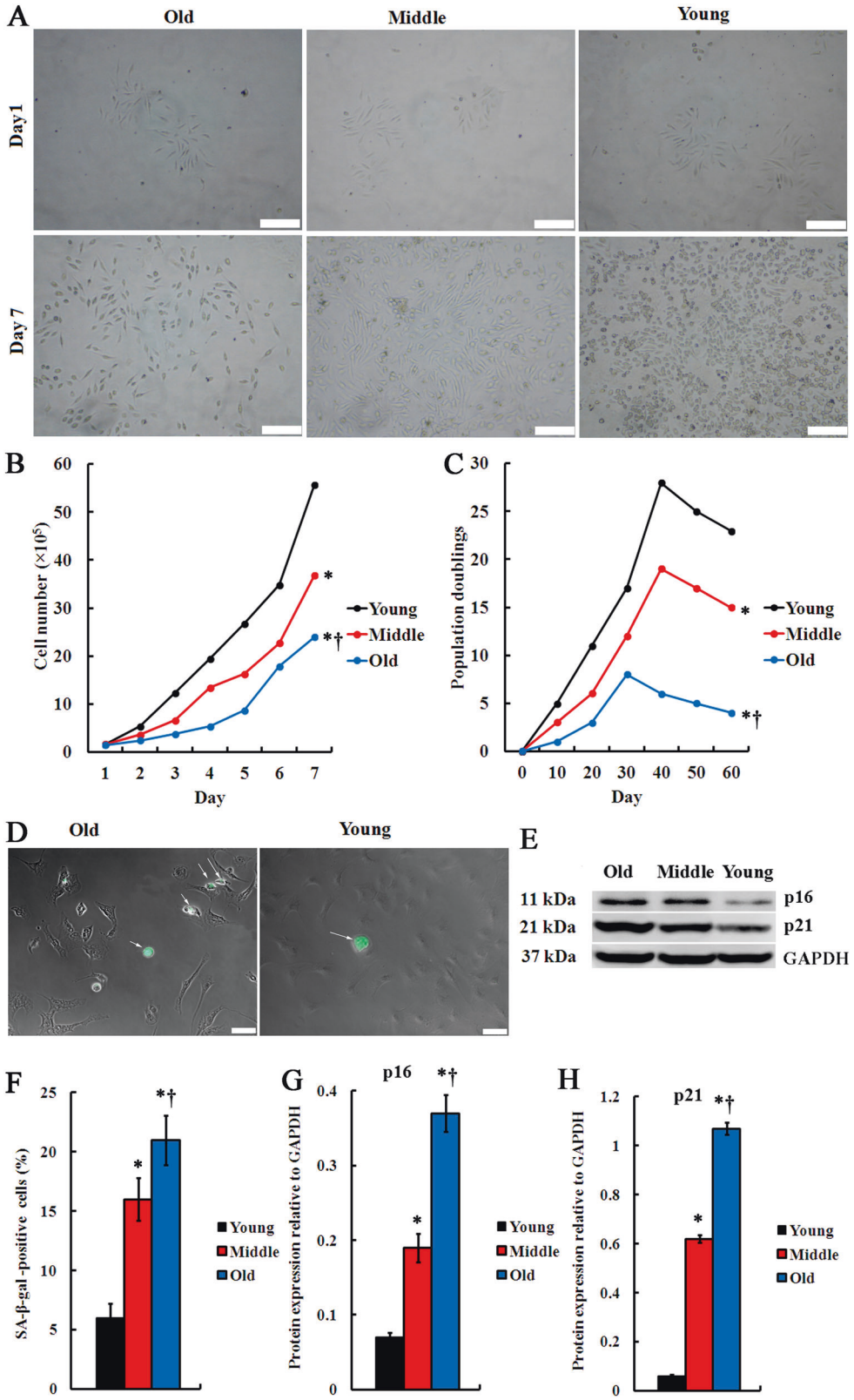

Fig. 2 (Continued)

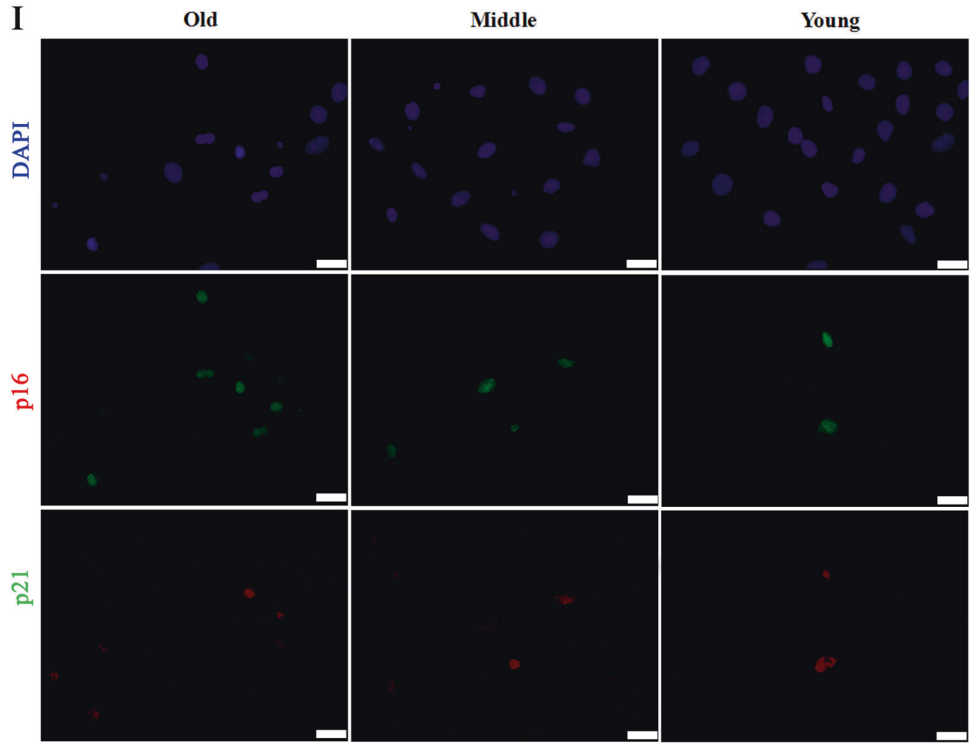

Fig. 2 Aging decreased the lifespan of primary cultured human $CD133^+/VEGFR2^+$ cells. **a** Representative growth state and morphology of the $CD133^+/VEGFR2^+$ cells from the young, middle-aged, and old patients at the early stages (day 1, day 7) of culture. Scale bars = 20 μm. **b** Human $CD133^+/VEGFR2^+$ cells from patients of the three age were cultured for 7 days and seeded at a density of 3×10^5 cells per 100 mm plate on day 0. Cell number per 100 mm plate was then counted at indicated time points. $p < 0.05$: *vs. young group, †vs. middle-aged group ($n = 10$ in each group). **c** Human EPCs were passaged until they underwent senescence, and the number of cumulative population doublings was determined. **d** Cell morphology senescence-associated β-galactosidase staining (white arrowheads) in EPCs from the old and the young patients. Scale bars = 50 μm. **e** Whole-cell lysates (30 μg) of the old, middle-aged, and young $CD133^+/VEGFR2^+$ cells on day 60 were examined for the expression of the senescence markers, p16 and p21, and GAPDH (loading control) by Western blotting. **f** Statistical analysis of the mean percentage of β-galactosidase-positive cells relative to the whole $CD133^+/VEGFR2^+$ cells. **g**, **h** The levels of p16 and p21 proteins relative to GAPDH expression. $p < 0.05$: *vs. young group, †vs. middle-aged group ($n = 10$ in each group). **i** p16 and p21 expression in cells determined by immunofluorescence with anti-p16 (green) and anti-p21 (red) antibodies, respectively. Nuclei were counterstained with DAPI (4′,6-diamidino-2-phenylindole). Bars = 50 μm. p16 and p21 were mainly localized in the nucleus. The expression of p16 and p21 were markedly higher in the old $CD133^+/VEGFR2^+$ cells than in the young $CD133^+/VEGFR2^+$ cells. These data all indicate increased senescence of $CD133^+/VEGFR2^+$ cells from elderly patients

induction specifically targets GDF11, we performed western blotting and ELISAs to investigate the protein expression of other TGF-β proteins, activin and myostatin, in addition to GDF11 in old $VEGFR2^+/CD133^+$ cells that did or did not receive adTERT. We observed a significant increase of GDF11 expression in old $VEGFR2^+/CD133^+$ cells receiving adTERT (adTERT) compared with those receiving vehicle, while transfection of adTERT did not cause a significant increase in the expression of myostatin and activin (Fig. S4A and S4B), suggesting that TERT is the sole/primary regulator of GDF11 in old $VEGFR2^+/CD133^+$ cells.

We then investigated the mechanism by which TERT controls GDF11-mediated rejuvenation of old $VEGFR2^+/CD133^+$ cells. We found mRNA and protein levels of GDF11 and TERT were significantly upregulated in TERT-overexpressing $VEGFR2^+/CD133^+$ cells and that both GDF11 and TERT were downregulated by TERT depletion (Fig. 4e–g). We also showed that addition of rhGDF11 did not affect TERT expression in $VEGFR2^+/CD133^+$ cells (Fig. 4f, g). Consistent with the changes in TERT expression, there were similar changes in telomerase expression in older $VEGFR2^+/CD133^+$ cells after adding rhGDF11, adTERT, or siTERT (Fig. 4h). GDF11 was mainly expressed in the cytoplasm, particularly in the perinuclear region, and TERT was mainly expressed in the nuclei and perinuclear. When treated with adTERT, with or without rhGDF11, the staining intensity of both GDF11 and TERT markedly increased, while siTERT suppressed the staining intensity. Addition of rhGDF11 did not distinctly affect the expression of TERT (Fig. 4i). Together these data indicate that TERT overexpression activates GDF11 signaling. Because hypoxia leads to a further reduced number of $VEGFR2^+/CD133^+$ cells, we assessed how TERT and

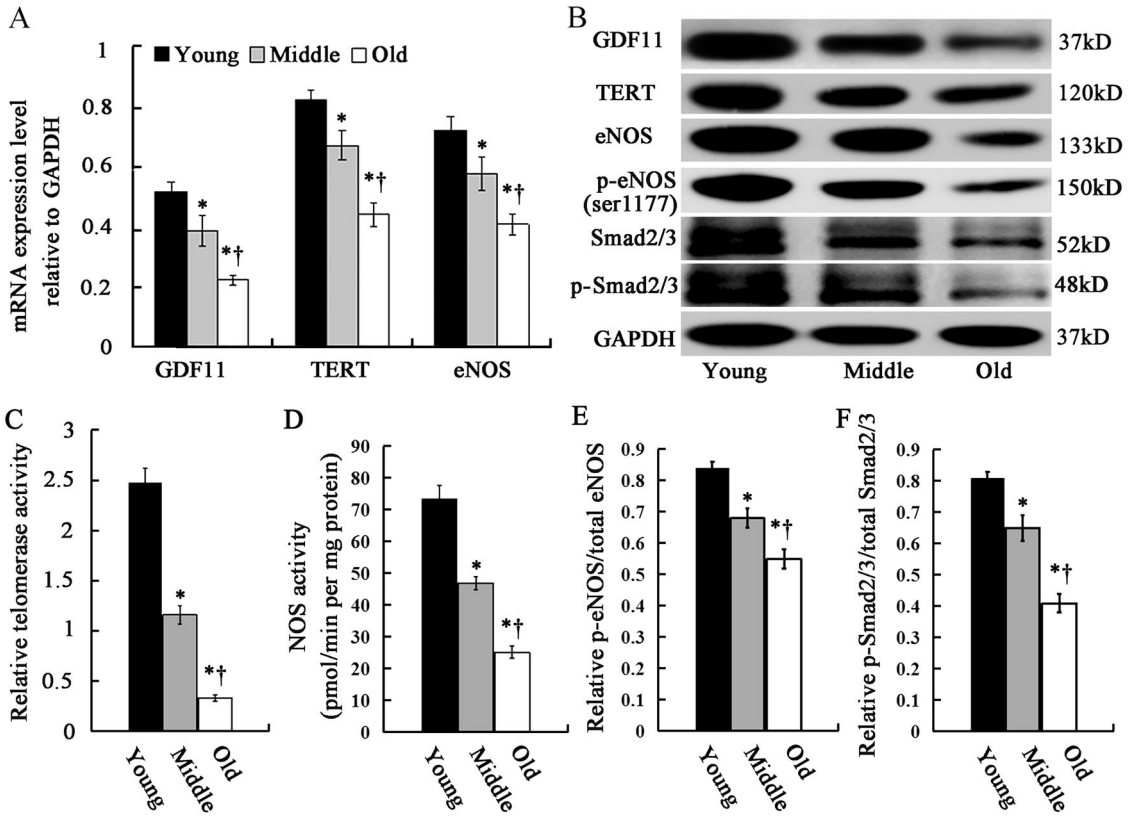

Fig. 3 Aging affected expression of TERT and GDF11-mediated signalings. **a** qRT-PCR measurements of gene expression levels of GDF11, TERT, and eNOS of $CD133^+/VEGFR2^+$ cells from the young, middle-aged, and old patients, respectively. **b** Representative western blots of the protein levels of GDF11, TERT, eNOS, Smad2/3, and phosphorylation of eNOS and Smad2/3 in the $CD133^+/VEGFR2^+$ cells from the three age patients. **c**, **d** The difference of telomerase activity (**c**) and eNOS activity (**d**) between $CD133^+/VEGFR2^+$ cells. **e**, **f** Phosphorylation levels of eNOS (**e**) and Smad2/3 (**f**) in these cells. All data represent means ± s.e.m. $p < 0.05$: *vs. young group, †vs. middle-aged group ($n = 10$ in each group). The expression levels of TERT and GDF11-relative signaling markedly declined in the $CD133^+/VEGFR2^+$ cells with age

GDF11 could affect the older cell populations by analyzing the apoptotic cells and proliferative Ki-67^+ cells. Under hypoxic conditions, 23–31% of old $VEGFR2^+/CD133^+$ cells underwent apoptosis (Fig. 4j). GDF11 caused only mild decrease of the apoptosis rate, while adTERT significantly decreased the rate. Co-administration of rhGDF11 and adTERT resulted in further decreased apoptosis levels of $VEGFR2^+/CD133^+$ cells. However, siTERT, with or without rhGDF11, significantly abrogated this decrease. Quantification of proliferation revealed a 1.4-fold increase in Ki-67^+ cells in the adTERT-treated cells, and a 2.0-fold increase in Ki-67^+ cells in the cells co-treated with adTERT and GDF11 compared with the control without GDF11 or TERT. However, these cell populations were unaffected by addition of GDF11 alone (Fig. 4k). These data demonstrate that TERT can promote the anti-apoptotic and proliferative potential of aged $VEGFR2^+/CD133^+$ cells under hypoxia.

We then analyzed the role of TERT in GDF11-mediated rejuvenation of older $VEGFR2^+/CD133^+$ cells. TERT could significantly increase telomerase activity in older EPCs. We also tested the ability of TERT to activate rhGDF11-associated anti-senescence effect. Under hypoxia, long-term culture studies showed that adTERT significantly extended the lifespan of EPCs, and co-overexpressing TERT and GDF11 further promoted cell lifespan. However, siTERT led to a greater decrease in lifespan, and adding GDF11 alone did not cause a significant extension of cell lifespan (Fig. 4l). TERT significantly decreased the SA-β-gal activity of $VEGFR2^+/CD133^+$ cells, with maximal inhibitory effect achieved in $VEGFR2^+/CD133^+$ cells co-treated with rhGDF11 and adTERT. Conversely, siTERT significantly increased the SA-β-gal activity. However, an obvious decrease in SA-β-gal activity was not observed in the cells receiving simple GDF11 treatment, which had lower expression of TERT (Fig. 4m), suggesting that TERT controls the GDF11-mediated rejuvenation of senescent $VEGFR2^+/CD133^+$ cells from older patients.

TERT controls GDF11-mediated canonical signaling

We used SB431542 (10 μmol/L, a Smad2/3 inhibitor) to determine whether GDF11-mediated regulation of Smad2/3

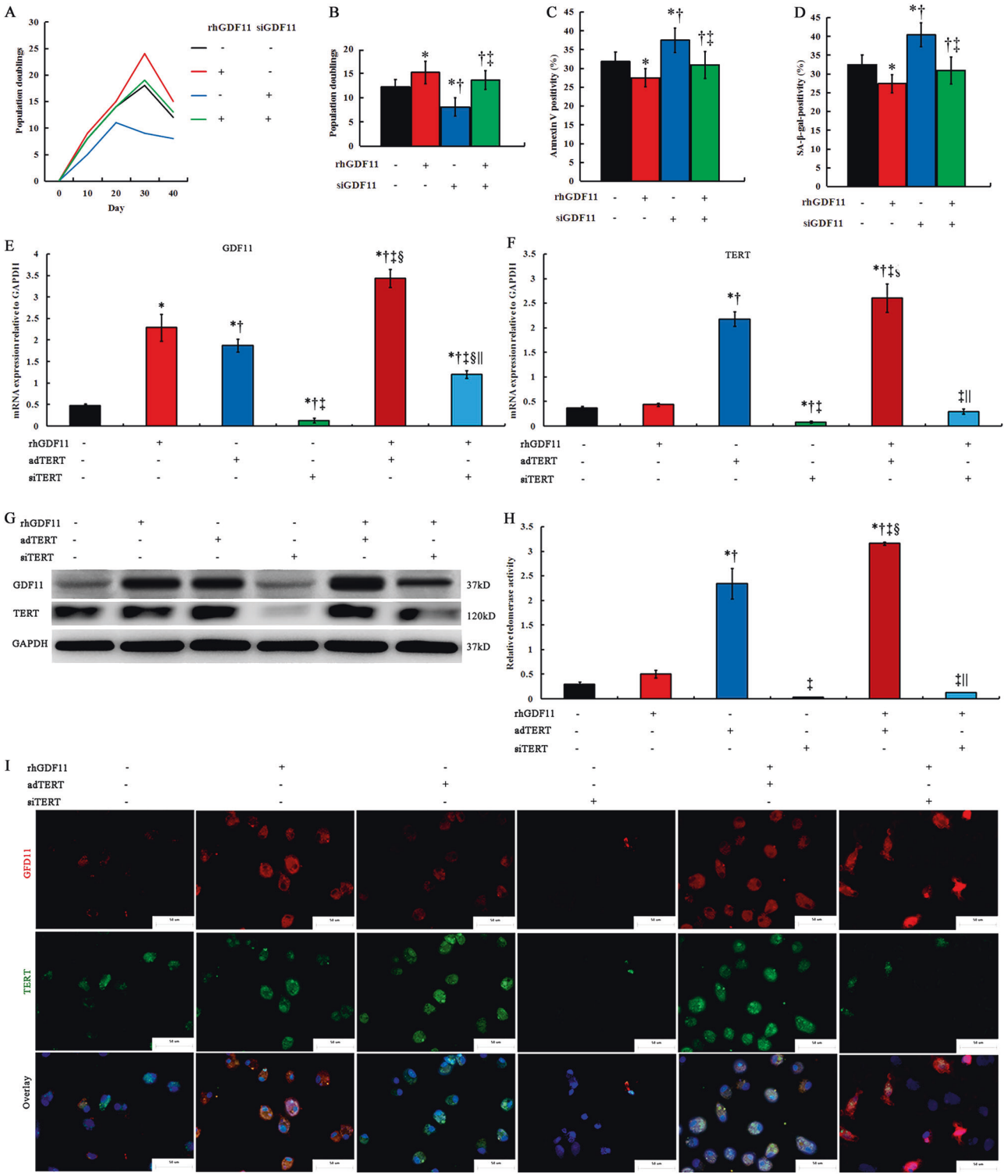

Fig. 4 (Continued)

activity is dependent on TERT. Immunoblot analysis showed that rhGDF11 stimulation increased Smad2/3 activity compared with null treatment (WT); treating cells with adTERT activated the Smad2/3 signaling pathway, revealed by a significant increase in the Smad2/3 phosphorylation cascade, and rhGDF11 and adTERT treatment further increased Smad2/3 phosphorylation cascade, which was prevented by adding SB431542 (Fig. 5a–c). We then determined whether rhGDF11 activation of Smad2/3 exerts transcriptional effects specific to

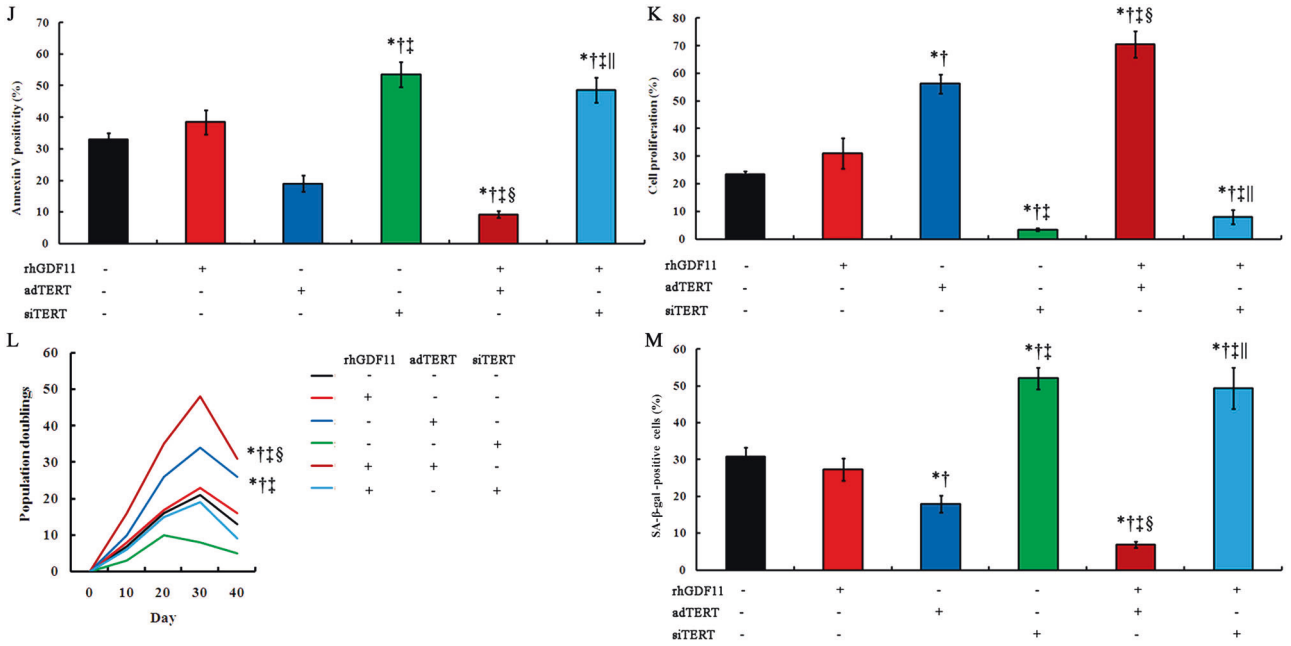

Fig. 4 TERT improved GDF11-mediated rejuvenation of old CD133$^+$/VEGFR2$^+$ cells. **a** The number of cumulative population doublings of old CD133$^+$/VEGFR2$^+$ cells in the presence or absence of rhGDF11 or siGDF11 under long-term hypoxic culture. **b–d** The number of cumulative population doublings (**b**), FACS analysis of annexin V/propidium iodide (**c**), and quantification of the senescence assays using β-galactosidase staining (**d**), were determined in old CD133$^+$/VEGFR2$^+$ cells receiving rhGDF11 or siGDF11 under long-term hypoxic culture. All data represent means ± SD. $p < 0.05$: *vs. vehicle, †vs. rhGDF11 adding, and ‡vs. siGDF11 adding ($n = 10$ per group). Afterward, old CD133$^+$/VEGFR2$^+$ cells were transfected with vectors encoding TERT (adTERT) or TERT siRNA (siTERT) in the presence or absence of recombinant human GDF11 (rhGDF11) under hypoxic conditions. **e**, **f** qRT-PCR analysis of the mRNA and protein expression of GDF11 and TERT, respectively, under various conditions. **g** Western blot analysis of protein expression of GDF11 and TERT under various conditions. **h** Differences in telomerase activity. **i** GDF11 and TERT expression in cells determined by immunofluorescence with anti-GDF11 (red) and anti-TERT (green) antibodies, respectively. Also shown are DAPI staining (nuclei; blue) and merged images. Scale bars = 50 μm. **j** Cell death was evaluated via FACS analysis of annexin V/propidium iodide. **k** Cell proliferation was assessed by FACS analysis of Ki-67-positive cells, showing the greatest positive staining in the rhGDF11 + adTERT group, the second highest in the group receiving adTERT alone, and the leatest in the group treated with siTERT. **l** Number of cumulative population doublings under long-term hypoxic culture. **m** Quantification of the senescent assays using β-galactosidase staining. All data represent means ± s.e.m. $p < 0.05$: *vs. vehicle, †vs. rhGDF11 adding, ‡vs. adTERT adding, §vs. siTERT adding, and $^{\|}$vs. rhGDF11 and adTERT adding ($n = 10$ per group)

the apoptosis network. Western blot analysis showed increased protein expression of the anti-apoptotic gene Bcl2 in TERT-overexpressing VEGFR2$^+$/CD133$^+$ cells treated with rhGDF11 compared with controls and the cells treated with rhGDF11 alone (Fig. 5a, d). Expression of the apoptotic gene caspase 3 showed the opposite trend: it was downregulated in TERT-overexpressing cells. However, these effects could be blocked by coincubation with SB431542 (Fig. 5a, e). Importantly, the change of Bcl2 expression was consistent with p-Smad2/3 expression after the treatment of rhGDF11, adTERT, and SB431542 (Fig. 5a, d). Therefore, these results identify Bcl2 as a direct phosphorylation substrate of Smad2/3 and demonstrate that TERT is an indispensable activator of such phosphorylation. Immunofluorescence analyses showed that double-positive staining for Smad2/3 and Bcl2 was the highest in cells that received rhGDF11 and adTERT, lower in cells that received adTERT treatment alone, and lowest in the cells treated with SB431542. More importantly, rhGDF11 stimulation of adTERT-treated cells resulted in Smad2/3 nucleus-to-cytosol translocation, which was prevented by incubation with the Smad2/3 inhibitor SB431542. Furthermore, the addition of rhGDF11 caused Smad2/3 to translocate into the nucleus (Fig. 5f). Thus, TERT activity is required for Smad2/3 cytosolic localization on GDF11 stimulation.

TERT and GDF11 rejuvenate neovascularization of older VEGFR2$^+$/CD133$^+$ cells via eNOS signaling

We explored the noncanonical signaling pathway of GDF11 in our study. Nitric oxide (NO), produced by eNOS, may improve the function of EPCs in disease [31]. We found no significant increase in the protein levels of NO or eNOS, and NOS activity under hypoxic conditions in VEGFR2$^+$/CD133$^+$ cells treated with GDF11 alone compared with

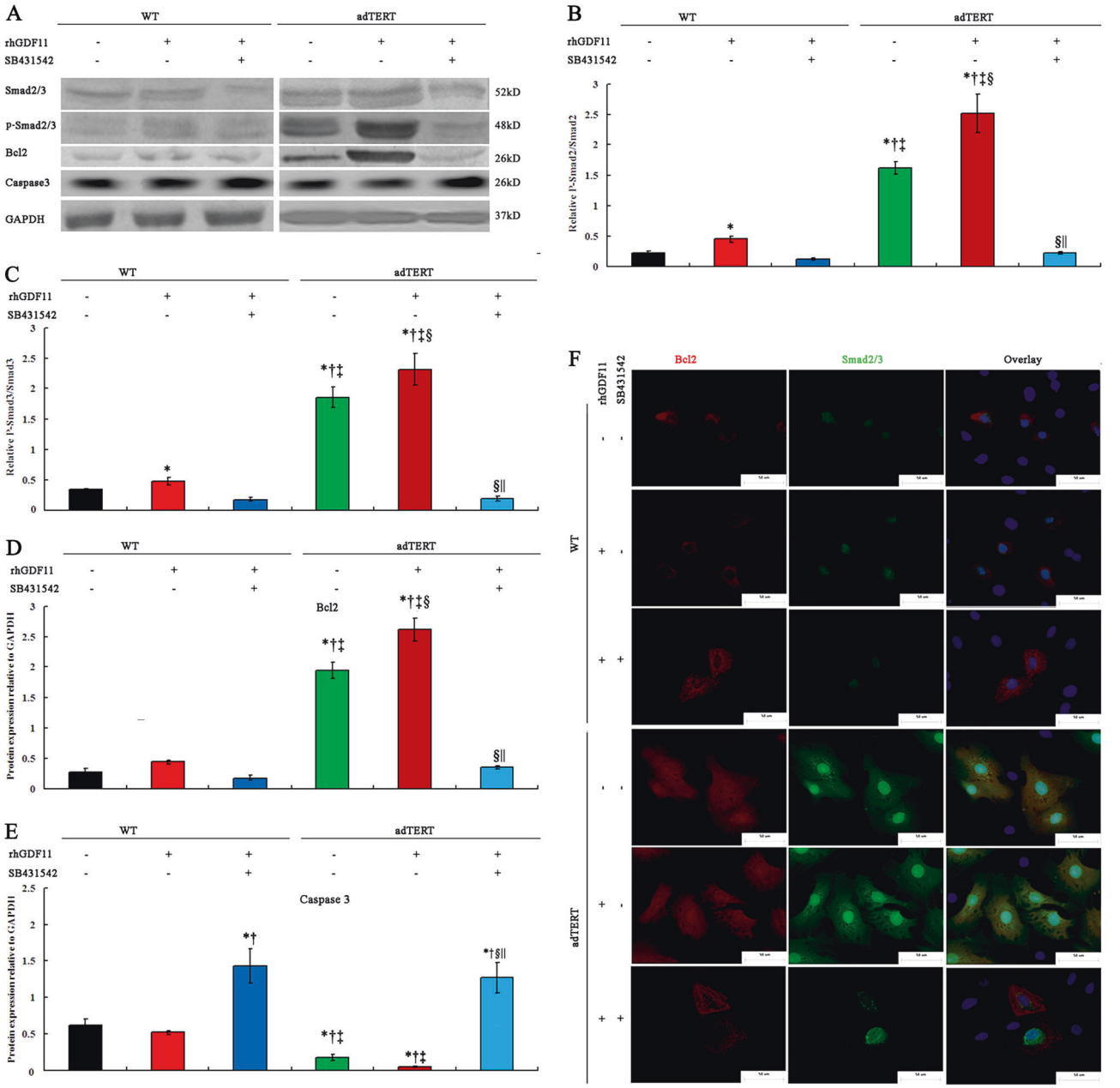

Fig. 5 TERT promoted GDF11 activation of Smad2/3 signaling in old $CD133^+/VEGFR2^+$ cells. **a–e** Western blot analysis of Smad2/3, Bcl2, and caspase 3 protein expression under various conditions. **a** Representative western blots of the protein levels of Smad2/3, Bcl2, caspase 3, and phosphorylation of eNOS and Smad2/3 in the $CD133^+/VEGFR2^+$ cells receiving rhGDF11, SB431542, or adTERT. **b–e** Quantitative analysis of expression of phosphorylated Smad2/3 (**b**, **c**), Bcl2 (**d**), and caspase 3 (**e**) in cells pre-transfected with vehicle (WT) or adTERT (adTERT) plus rhGDF11 or SB431542. All data represent means ± s.e.m. $p < 0.05$: *vs. vehicle, †vs. rhGDF11 addition, ‡vs. rhGDF1and SB431542 addition, §vs. adTERT addition, ||vs. rhGDF11 and adTERT addition ($n = 10$ per group). **f** $CD133^+/VEGFR2^+$ cells transfected with vehicle or adTERT were treated for 24 h with rhGDF11 or SB431542 before immunofluorescence labeling of Bcl2 (red) and Smad2/3 (green). DAPI indicates the nucleus of cells. Scale bars = 50 μm

control; however, a significant increase was observed in the TERT-overexpressing cells, with a further increase seen with both TERT and GDF11 overexpression. Conversely, NO and eNOS protein levels, and NOS activity in TERT-deficient cells, with or without GDF11 treatment, were similar and generally lower than those in controls (Fig. 6a–c). Western blot results showed that overexpression of TERT-induced phosphorylation of eNOS at Ser-1177. The addition of GDF11 further strengthened this phosphorylation, whereas TERT knockdown reduced eNOS phosphorylation (Fig. 6d, e). We also monitored neovascularization in $VEGFR2^+/CD133^+$ cells treated with

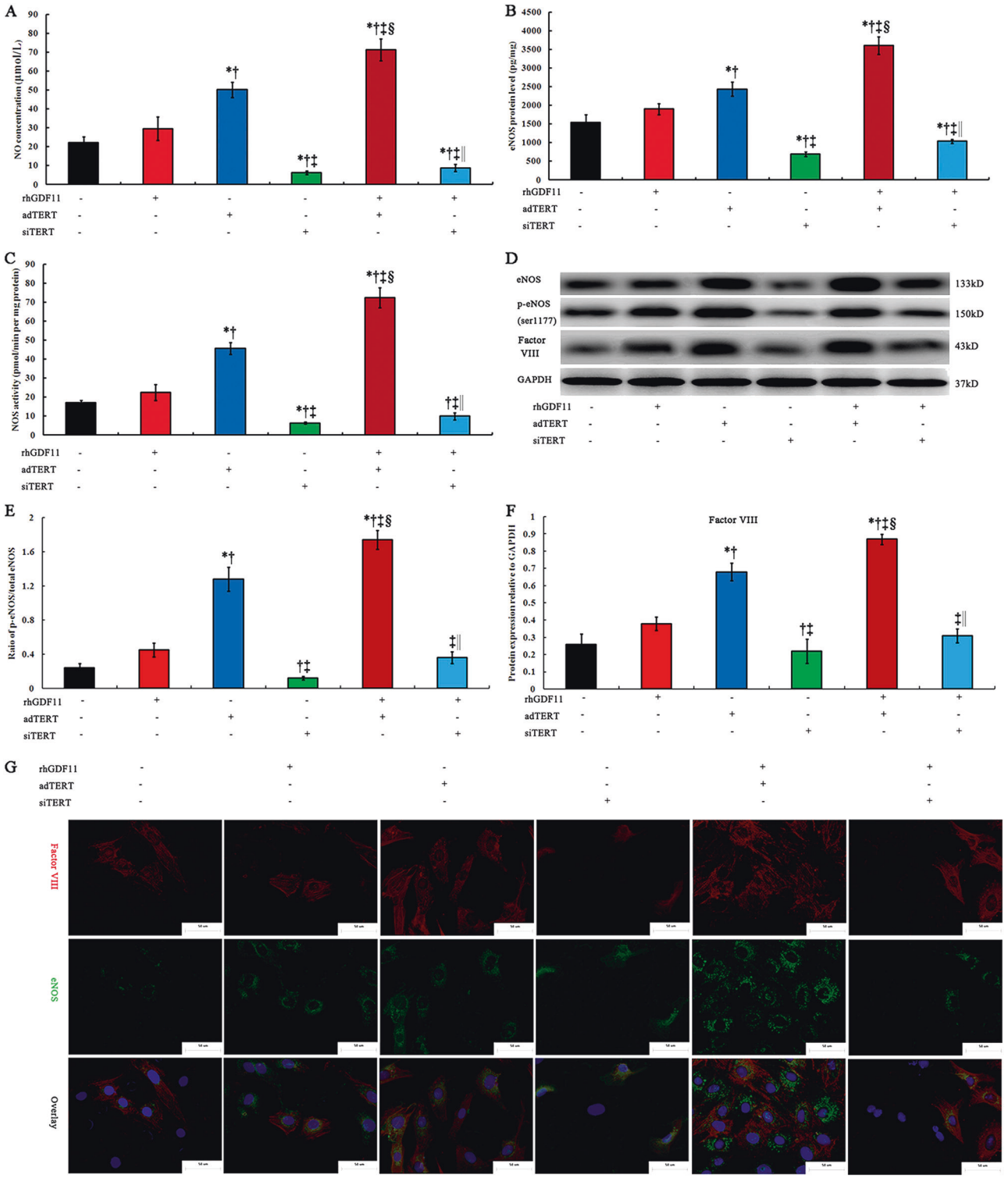

Fig. 6 (Continued)

growth factors to induce differentiation. In vitro vasculogenic potential of older EPCs was elucidated by assessing expression of the vascular endothelial marker protein factor VIII, secretion of angiogenic cytokines [11], and Matrigel assay [32]. Western blot showed that expression of factor VIII was highest in TERT-overexpressing VEGFR2^{+}/CD133^{+} cells with rhGDF11 added, and was significantly lower in TERT-deficient cells, with or without rhGDF11 (Fig. 6d, f). Our immunofluorescence experiments revealed that TERT transfection, alone or together with GDF11, was

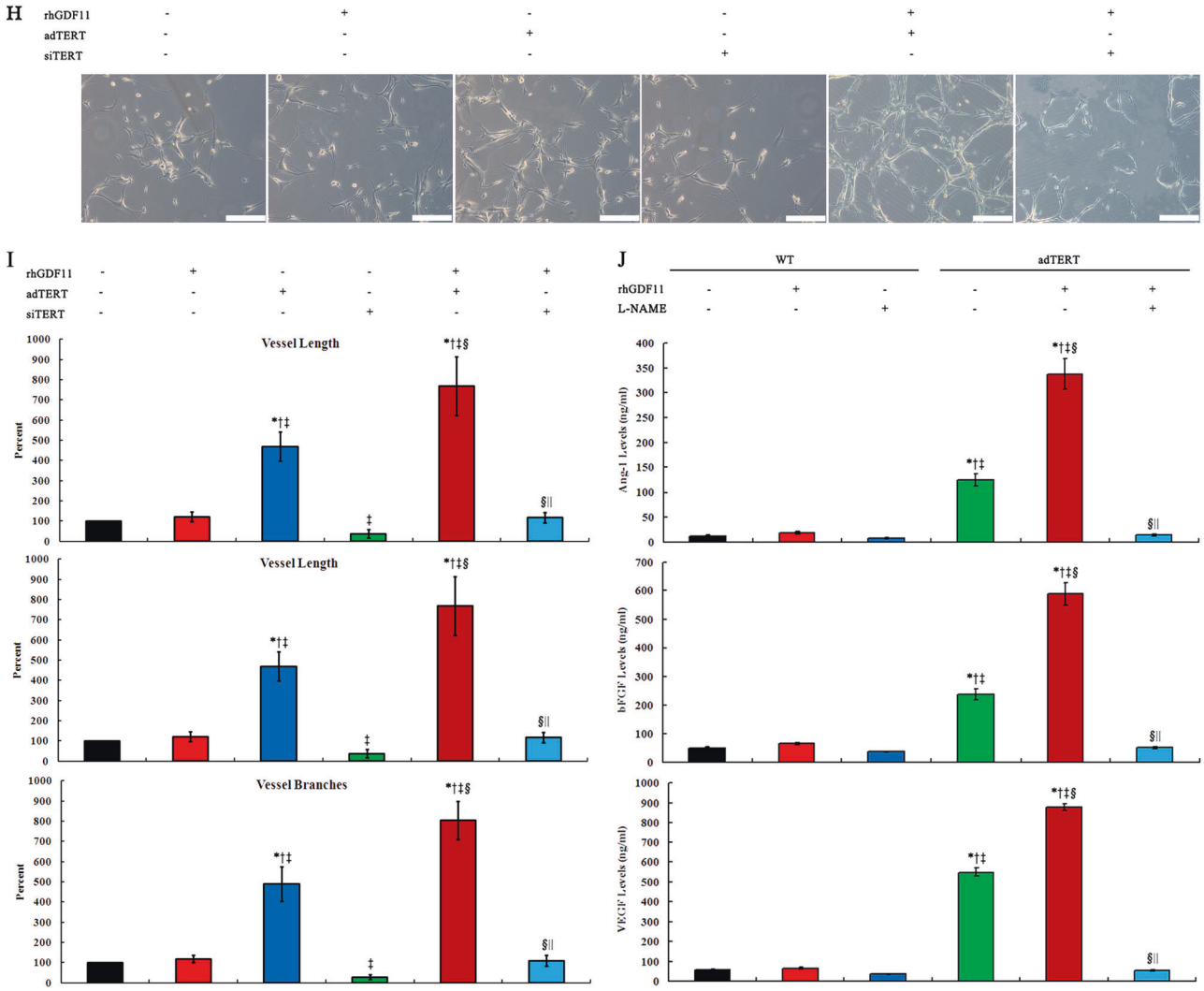

Fig. 6 TERT facilitated GDF11 to activate eNOS signaling pathways in old CD133$^+$/VEGFR2$^+$ cells. **a–c** Quantitative analysis of NO concentration (**a**), eNOS protein level (**b**), and NOS activity (**c**) in the old CD133$^+$/VEGFR2$^+$ cells transfected with vectors encoding TERT (adTERT) or TERT siRNA (siTERT) in the presence or absence of rhGDF11 under hypoxic conditions. **d** Representative western blots of the p-eNOS and factor VIII protein levels in old EPCs in the different groups (data represent at least three independent experiments). **e**, **f** Quantitative analysis of expression of eNOS phosphorylation (**e**) and factor VIII (**f**) determined by western blot in old CD133$^+$/VEGFR2$^+$ cells in the various groups. All data represent means ± s.e.m. $p < 0.05$: *vs. vehicle, †5 vs. rhGDF11 addition, ‡vs. adTERT addition, §vs. siTERT addition, $^{\|}$vs. rhGDF11 and adTERT addition ($n = 10$ per group). **g** Factor VIII and eNOS expression in cells determined by immunofluorescence with anti-factor VIII (red) and anti-eNOS (green) antibodies, respectively. Also shown are DAPI staining (nuclei; blue) and merged images. Scale bars = 50 μm. **h** Representative images showing enhanced angiogenesis in the presence of adTERT addition or both adTERT and rhGDF11 addition compared with other groups. Scale bars = 50 μm. **i** A statistically significant increase in vessel number, length, and branches presented as percentage of vehicle was evident with the cells adding adTERT or adding adTERT and rhGDF11 compared with the vehicle, addition of rhGDF11 alone, or addition of siTERT. **j** Quantitative analysis of Ang-1, bFGF, and VEGF proteins levels measured by ELISA in supernatant of the old CD133$^+$/VEGFR2$^+$ cells transfected with adTERT or empty vector (WT) post treatments of rhGDF11 or L-NAME (an eNOS inhibitor, 500 μmol/l). Data were shown as means ± s.e.m. $p < 0.05$: *vs. without any treatment in WT group, †vs. rhGDF11 addition in WT group, ‡vs. L-NAME addition in WT group, §vs. untreated controls in adTERT group, $^{\|}$vs. rhGDF11 addition in adTERT group ($n =$ 10 per group)

associated with notable increases in the number of VEGFR2$^+$/CD133$^+$ cells that expressed factor VIII and eNOS, while TERT knockdown reduced their prevalence (Fig. 6g). Matrigel tube formation was observed as reported by Atluri et al. [32] or Hermansen et al. [33]. The same effect on tubule formation was also seen in the Matrigel assay (Fig. 6h). There was a profound increase in vessel formation, vessel length, and branch formation with transfection of adTERT. As expected, there was minimal vasculogenesis evident with either media alone or rhGDF11 alone. Co-treatment with rhGDF11 and adTERT seems to increase the direct vasculogenic potential of older VEGFR2$^+$/CD133$^+$ cells, whereas siTERT significantly decreased this vasculogenic potential. A statistically

significant increase in vessel formation, vessel length, and branch formation was demonstrated with adTERT and rhGDF11 compared with the adTERT or rhGDF11 groups (Fig. 6i). This in vitro assay demonstrates significant direct EPC-mediated angiogenic potential after receiving adTERT and rhGDF11. The supernatant levels of Ang-1, bFGF, and VEGF in VEGFR2$^+$/CD133$^+$ cells were detected to evaluate the secretion function of older VEGFR2$^+$/CD133$^+$ cells by ELISA. Finally, we measured the production of proangiogenic cytokines in supernatant of VEGFR2$^+$/CD133$^+$ cells after treatment with L-NAME (an eNOS inhibitor). As expected, L-NAME significantly inhibited GDF11 or TERT-induced overexpression of proangiogenic cytokines, including Ang-1, bFGF, and VEGF (Fig. 6j). This suggested that the rejuvenation of TERT-dependent GDF11 likely occurs by inducing eNOS signaling and secretion of proangiogenic factors.

TERT depletion causes senescence of young VEGFR2$^+$/CD133$^+$ cells

Next, we determined whether loss of GDF11 or TERT by addition of the GDF11 antagonist follistatin or TERT knockdown, respectively, could cause aging in young VEGFR2$^+$/CD133$^+$ cells. The protein levels of TERT and GDF11 were significantly downregulated in young VEGFR2$^+$/CD133$^+$ cells following follistatin treatment or siTERT transfection. The level of TERT decline caused by follistatin is not as significant as that due to siTERT. Follistatin treatment or siTERT transfection caused similar decreases in the protein expression levels of Smad2/3-relative anti-apoptotic protein Bcl2 and eNOS-related vascular growth factors Ang-1, bFGF, and VEGF in comparison with untreated controls (Fig. 7a). We then tested the proliferative and anti-apoptotic potential of young VEGFR2$^+$/CD133$^+$ cells by Ki-67 immunofluorescence and TUNEL staining. Follistatin or siTERT markedly attenuated cell proliferation compared with untreated controls (Fig. 7b). Follistatin or TERT depletion caused a significant increase in the apoptotic rate of young VEGFR2$^+$/CD133$^+$ cells while compared with untreated controls (Fig. 7c). This suggests silencing of endogenous GDF11 or TERT induces the downregulation of anti-apoptotic genes by inhibiting their signaling pathways, thereby decreasing the sensitivity of young VEGFR2$^+$/CD133$^+$ cells to hypoxia. The colonies derived from follistatin-treated VEGFR2$^+$/CD133$^+$ cells or siTERT-treated cells were strikingly smaller and contained fewer cells than controls (Fig. 7d, f). We also found the ability for follistatin-treated cells or siTERT-treated cells to form capillary-like structures in a Matrigel matrix was significantly reduced compared with control VEGFR2$^+$/CD133$^+$ cells (Fig. 7e, g), and the migration presented out the same change trend in the young cells receiving follistatin or TERT knockdown (Fig. 7h). Neovascularization by assessing expression of factor VIII was significantly lower in the young EPCs treated with follistatin or siTERT than in control EPCs (Fig. 7i). Immunofluorescence showed that the expression of factor VIII was significantly reduced in both follistatin-treated EPCs or siTERT-treated EPCs compared with control EPCs (Fig. 7j). These studies confirm that depletion of GDF11 or TERT causes senescence in vascular endothelial function and angiogenesis of young EPCs.

Next, we observed the effects of follistatin, GDF knockdown, or TERT knockdown on the expression of senescence markers in young EPCs. The expression of senescence markers p21 and p16 was increased in VEGFR2$^+$/CD133$^+$ cells treated with siTERT or follistatin compared with control cells (Fig. 8a). In order to confirm TERT control of GDF11-mediated rejuvenation of VEGFR2$^+$/CD133$^+$ cells, we depleted TERT or GDF11 by siRNA-mediated knockdown, and rescued TERT or GDF11 by adTERT or rhGDF11 in young VEGFR2$^+$/CD133$^+$ cells. As shown in Fig. 8b, siGDF11 treatment resulted in increases in both p16 and p21, which was significantly weakened by rhGDF11 treatment and was further reduced by adTERT treatment. These data suggested that depletion of TERT or GDF11 caused senescence of young VEGFR2$^+$/CD133$^+$ cells, and overexpression of GDF11 or TERT rescued this senescence, and TERT played a more important role. In a direct comparison test of the effects of siTERT and GDF11 depletion on senescence of young VEGFR2$^+$/CD133$^+$ cells, ELISA assay was used to assess p16 and p21 levels. siGDF11 led to the similar increase in p16 and p21 expression with follistatin, and siTERT caused higher increase in the expression of p16 and p21 than follistatin and siGDF11. This increase was significantly weakened by rhGDF11 treatment, and was further reduced by adTERT treatment (Fig. 8c, d). These data further confirmed that depletion of GDF11 caused senescence of young EPCs, and addition of rhGDF11 or adTERT rescued this senescence. Moreover, a more significant decrease of p16 and p21 expression was seen in the siGDF11-treated cells receiving adTERT compared with that in the siTERT-treated cells receiving rhGDF11 (Fig. 8c, d), confirming that TERT causes better rejuvenation of VEGFR2$^+$/CD133$^+$ cells than GDF11. We then analyzed the different effects of follistatin and siGDF11 on senescence of young VEGFR2$^+$/CD133$^+$ cells. Statistical analysis revealed that the expression levels of p16 and p21 were slightly higher in cells receiving siGDF11 than in cells receiving follistatin (Fig. 8c, d).

In order to determine whether follistatin-mediated depletion of GDF11 is comparable with siRNA-mediated knockdown of GDF11, we performed western blot and ELISA to evaluate the changes in GDF11 protein

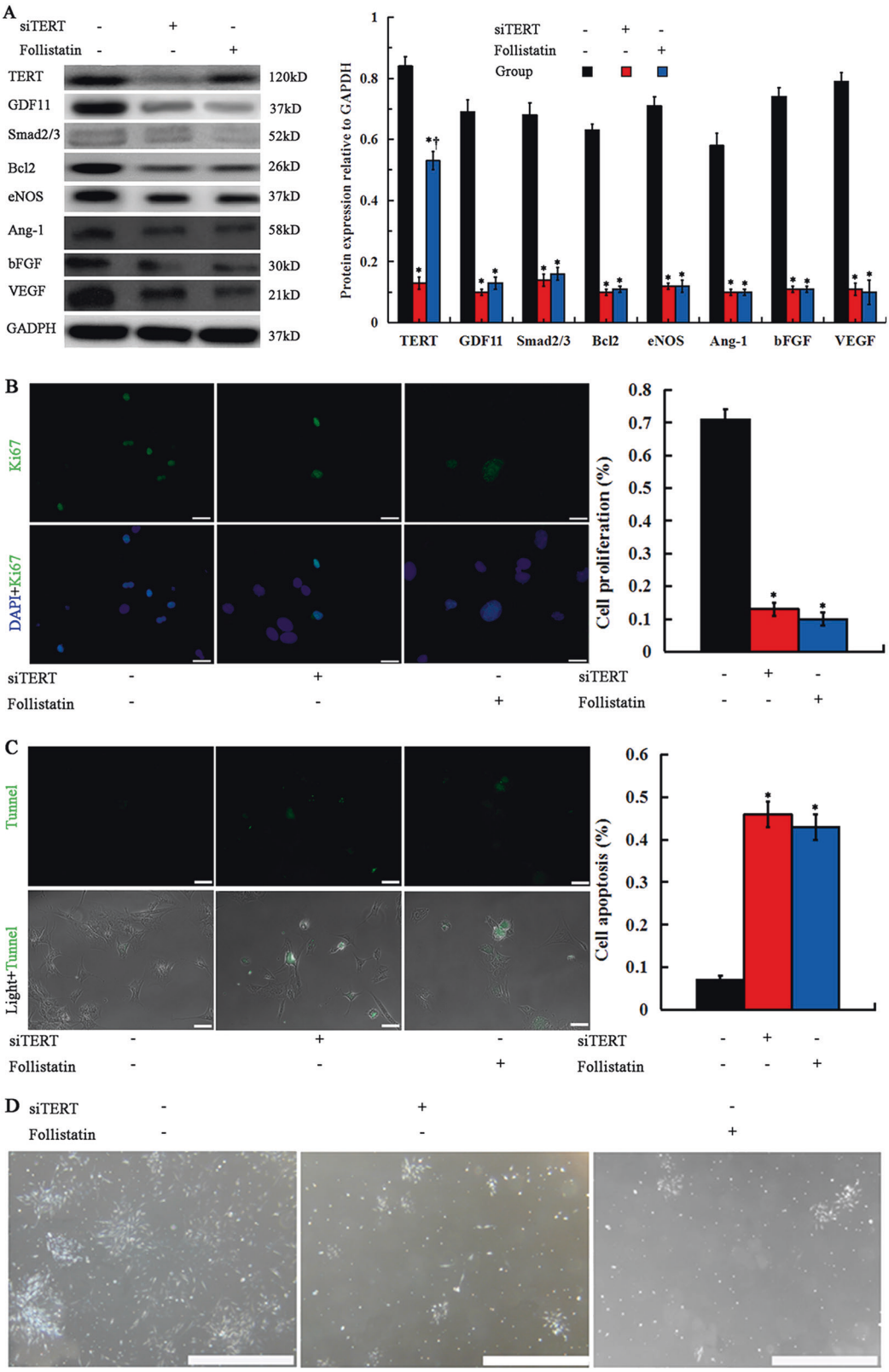

Fig. 7 (Continued)

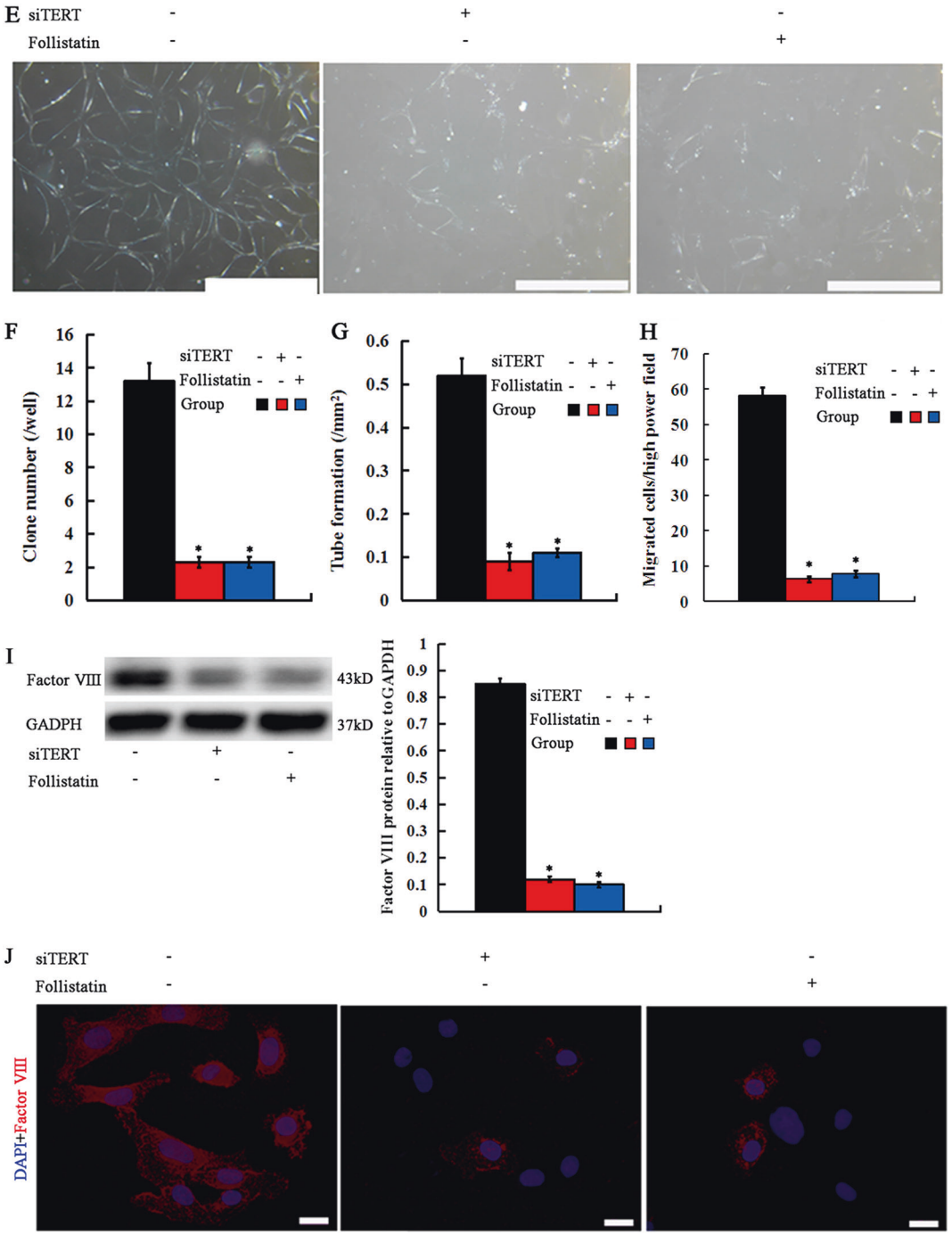

Fig. 7 Depletion of GDF11 or TERT caused senescence and impaired angiogenesis. **a** Western blot analysis of TERT, GDF11, Smad2/3, Bcl2, eNOS, Ang-1, bFGF, and VEGF protein expression in young $CD133^{+}/VEGFR2^{+}$ cells after depletion of GDF11 or TERT treated with follistatin or siTERT. **b** Immunofluorescence analysis of Ki-67 expressing cells (double stained with anti-Ki-67 and DAPI) in young $ECD133^{+}/VEGFR2^{+}$ cells after treatment with follistatin or siTERT. **c** Apoptosis analysis of young $CD133^{+}/VEGFR2^{+}$ cells by Tunnel staining after intervention of follistatin or siTERT. **d–g** Representative photomicrographs (**d**, **e**), quantitative analysis (**f**, **g**) of the colonies (**d**, **f**), and the tube formation (**e**, **g**) derived from a control (without treatment of follistatin or siTERT), follistatin-, or siTERT-cells. **h** The migration change of young $CD133^{+}/VEGFR2^{+}$ cells induced by follistatin or siTERT. **i** Western blot analysis of protein expression of Factor VIII in young $CD133^{+}/VEGFR2^{+}$ cells after depletion of GDF11 or TERT treated with follistatin or siTERT. **j** Cells were double-stained with DAPI (nuclei, blue) and anti-factor VIII (plasma, red) antibodies. Scale bars = 50 μm. All data are shown as means ± s.e.m. $p < 0.05$: *vs. untreated controls, †vs. siTERT treatment ($n = 10$ per group)

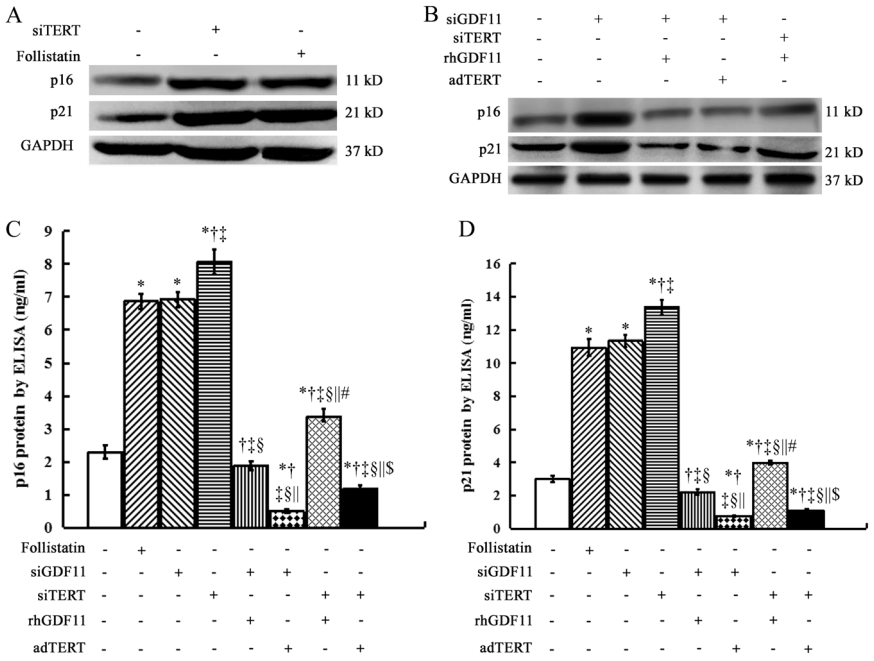

Fig. 8 siTERT, follistatin, siGDF11, and adTERT caused different expression of senescence proteins in young $CD133^+/VEGFR2^+$ cells. **a** Western blot analysis to determine siTERT versus follistatin induction of senescence proteins, p16 and p21. **b** Immunoblotting comparison of p16 and p21 expression in cells receiving siGDF11, siTERT, rhGDF11, or adTERT. GAPDH served as positive control. siGDF11 and siTERT stimulated expression of p16 and p21 in their sequence, while adTERT inhibited this senescence stimulation more than rhGDF11. **c**, **d** ELISA assay of difference in p16 and p21. Note that siTERT caused significantly higher increase in the expression of p16 and p21 than follistatin and siGDF11, and siGDF11 caused slight higher increase in p16 and p21 expression than follistatin. All data were shown as means ± s.e.m. $p < 0.05$: *vs. vehicle, †vs. follistatin addition, ‡vs. siGDF11 addition, §$p < 0.05$ vs. siTERT addition, ‖$p < 0.05$ vs. siGDF11 + rhGDF addition, #$p < 0.05$ vs. siGDF11 + adTERT, $p < 0.05$ vs. siTERT + rhGDF11 addition ($n = 10$ per group)

expression in young EPCs after treatment with follistatin or siGDF11. As expected, follistatin and siGDF11 caused significant decrease of GDF11 expression, but follistatin caused a lower degree of reduction than siGDF11 (Fig. S5A and S5B), suggesting that an siRNA-mediated knockdown of GDF11 would be more effective in senescence than the GDF11 antagonist follistatin. Thus, in the following experiments, we used siGDF11 instead of follistatin for GDF11 inhibition.

In order to further decipher the mechanisms of GDF11-mediated signaling in senescence of young $VEGFR2^+/CD133^+$ cells after depletion of GDF11 or TERT and the role of TERT in the process, we performed sequencing studies to investigate overall translation changes in GDF11-relative canonical (Smad2/3) and noncanonical (eNOS) signaling pathways resulting from GDF11 or TERT depletion. Western blot showed that compared with vehicle (CON), both siGDF11 and siTERT significantly decreased the expression of GDF11, eNOS, and Smad2/3; neither siGDF11 nor siTERT was capable of blocking other TGF-β family members, myostatin and BMP-4 (Fig. S6A). A human angiogenesis antibody array and a human apoptosis array were used to analyze the expression of GDF11-related noncanonical and canonical signaling factors from young $VEGFR2^+/CD133^+$ cells harvested under hypoxia in the deletion of TERT or GDF11. The arrays revealed that for some TGF-β family members, both siGDF11 and siTERT did not inhibit follastitin, activin A, and TGF-β1 (Fig. S6B). Hence, our results confirm that siGDF11 have a high degree of specificity for GDF11, and siTERT is the primary inhibitor of GDF11 in young $VEGFR2^+/CD133^+$ cells. For proangiogenic factors, Ang-1, bFGF, IGF-1, Tie-2, and VEGF were significantly decreased by *si*TERT or follistatin compared with null treatment (CON) (Fig. S6B). For anti-apoptotic signaling proteins, Bcl-2 and Survivin, siGDF11 or siTERT significantly decreased their expression compared with null treatment. Conversely, p21 and p27 were significantly increased by siGDF11 or siTERT, reflecting changes that would play a role in causing young $VEGFR2^+/CD133^+$ cell senescence. The expression of Bad, Bax, caspase 3, and caspase8 was significantly stimulated by siGDF11 or siTERT compared with null treatment (Fig. S6C). All these data further confirmed that GDF11 served as a sole regulator of canonical and noncanonical signaling in senescence of young $VEGFR2^+/CD133^+$ cells, and TERT induction specifically targets GDF11.

Depletion of GDF11 or TERT inhibits aged myocardial repair induced by young VEGFR2$^+$/CD133$^+$ cells

The capacity for cardiac ischemic repair and stem cell regenerative potential diminish with age [34]. Thus, we set out to confirm whether depletion of GDF11 or TERT directly caused senescence and impaired vascular function and angiogenesis of young EPCs by using an MI model of old rats by ligation of left anterior descending branch and transplantation of young VEGFR2$^+$/CD133$^+$ cells or EPCs (yEPC) pre-treated with vehicle, siGDF11, or siTERT. Injection of old VEGFR2$^+$/CD133$^+$ cells (oEPC) or PBS was used as controls. The 100 animals were randomly divided into five groups (Fig. S2). Thereafter, all animals were followed up for 30 days, during which 41 rats died. The surviving 59 rats underwent serial functional studies. After 30 days, Kaplan–Meier survival analysis showed a higher survival rate in the old MI rats receiving young VEGFR2$^+$/CD133$^+$ cell transplantation + vehicle than in other rats (85% in the rats receiving young VEGFR2$^+$/CD133$^+$ cells versus 50% in the rats receiving PBS, $p = 0.023$; 55% in the rats receiving old cells, $p = 0.04$; 50% in the rats receiving young EPCs + siTERT, $p = 0.028$; 55% in the rats receiving young EPCs + siGDF11, $p = 0.044$). However, siTERT and siGDF11 canceled these effects in young EPC-treated old rats (Fig. 9a).

Echocardiographic studies showed that the baseline (pre-MI, before MI induction; pre-Tx, before cell therapy) cardiac function index (LVFS, left-ventricular fractional shortening), LV remodeling indices (LVEDd [left-ventricular end-diastolic dimension], and LVEDv [left-ventricular end-diastolic volume]) were not significantly different among the groups. However, at 30 days, old rats that had received young VEGFR2$^+$/CD133$^+$ cells exhibited the greatest improvement in LVFS, LVEDd, and LVEDv, however, siTERT and siGDF11 eliminated these beneficial effects (Fig. 9b–d). Consistent with the changes in LV structure, LV weights in the young cells therapy group were significantly lower than those of the PBS and the old EPC therapy groups (1.95 ± 0.01 g/kg vs. 2.20 ± 0.02 g/kg and 2.09 ± 0.02 g/kg, respectively, $P < 0.01$), whereas there were no statistical significant differences between the PBS, oEPC, yEPC + siTERT, and yEPC + siGDF11 groups (Fig. 9e). Quantitative analysis of TTC staining showed that, compared with PBS or old EPC therapy alone, young EPC transplantation significantly reduced infarct size. However, siTERT or siGDF11 diminished this effect (Fig. 9f). These results indicate that depletion of GDF11 or TERT causes senescence of young VEGFR2$^+$/CD133$^+$ cells in aged myocardial function.

Depletion of GDF11 or TERT impaired angiogenesis and vascular function induced by young VEGFR2$^+$/CD133$^+$ cells in vivo

To determine the effects of siGDF11 or siTERT in angiogenesis and vascular function in the ischemic myocardium after young cell therapy, we measured proangiogenic factors Ang-1, bFGF, and VEGF, and the blood vascular density in the myocardium using real-time RT-PCR, western blot, and immunohistochemistry. At day 30, young VEGFR2$^+$/CD133$^+$ cell therapy induced an overall increase in the mRNA and protein expression of Ang-1, bFGF, and VEGF; siGDF11 or siTERT significantly decreased this response (Fig. 10a, b). Compared with old VEGFR2$^+$/CD133$^+$ cell therapy or PBS injection, simple transplantation of young VEGFR2$^+$/CD133$^+$ cells caused higher protein expression of GDF11 and TERT, siGDF11 significantly decreased their expression, and siTERT further enhanced this decrease (Fig. 10b). Immunohistochemistry showed that proangiogenic cytokines, e.g., Ang-1, were detected mainly in the vascular ECs and ischemic lesions in the old MI hearts treated with young EPCs, but their expression levels were significantly decreased in the MI hearts treated with siGDF11 or siTERT plus young EPCs, or old EPCs (Fig. 10f). Tissue sections were stained for anti-factor VIII antibody to detect ECs. yEPCs-treated old hearts had more blood vessels than the PBS- or oEPC-treated MI hearts, and siTERT or siGDF11 appeared to prevent this increase in vessel density (Fig. 10c, g). Collectively, these findings suggest that the initial depletion of TERT or GDF11 impaired angiogenesis and vascular secretion induced by young VEGFR2$^+$/CD133$^+$ cells in ischemic hearts.

We investigated the relationship between TERT-mediated GDF11 signaling and transplanted cell engraftment/vasculogenesis. FACS showed that EGFP-expressing cells were significantly more common in the yEPC group than in the oEPC group. However, siTERT or siGDF11 significantly decreased this engraftment (Fig. 10d, h). These data suggest that depletion of TERT or GDF11 might induce the loss of the young VEGFR2$^+$/CD133$^+$ cells engrafted into MI hearts during ischemia. The effect of siTERT or siGDF11 impairment on the vasculogenesis of the transplanted young VEGFR2$^+$/CD133$^+$ cells was evaluated by FACS and immunofluorescence in EGFP-positive cells isolated from the peri-infarct region. The young EPC old MI hearts had significantly higher factor VIII expression than the old VEGFR2$^+$/CD133$^+$ cells-treated old MI hearts, and siTERT or siGDF11 appeared to decrease factor VIII expression significantly (Fig. 10e, i, and j). Therefore, depletion of TERT or TERT impaired young VEGFR2$^+$/CD133$^+$ cell vasculogenesis in the ischemic hearts.

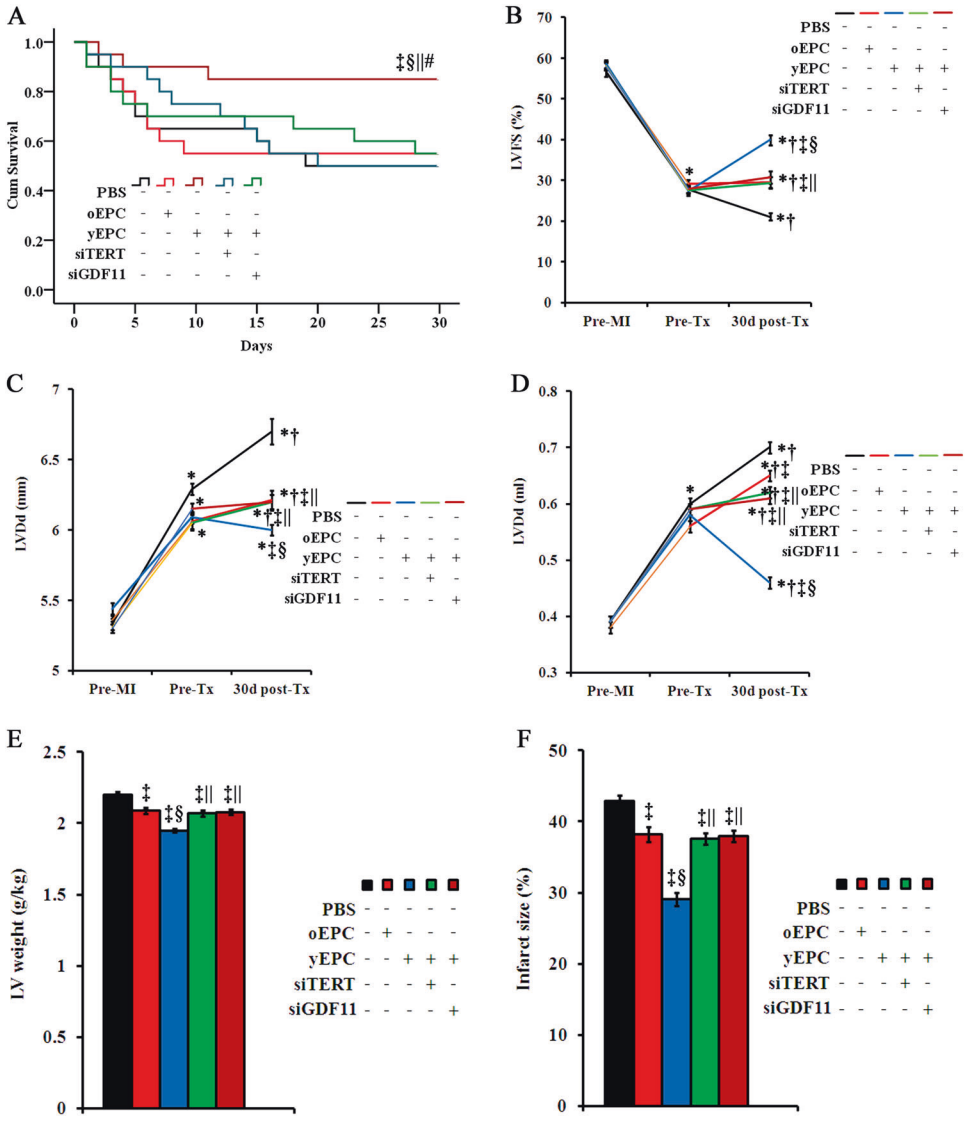

Fig. 9 Depletion of GDF11 or TERT-induced senescence of young CD133$^+$/VEGFR2$^+$ cells on aged myocardial repair. **a** Kaplan–Meier survival rates. **b–d** Echocardiography of LVFS (**b**), LVEDd (**c**), and LVEDv (**d**) before MI model (pre-MI), before cell treatment (pre-Tx), and before sacrifice post-cell transplantation (post-Tx). Young CD133$^+$/VEGFR2$^+$ cells-treated MI hearts had higher survival rates and significant improvement in cardiac function and structural remodeling, and siTERT or siGDF11 canceled this improvement. MI, myocardial infarction; Tx, transplantation. All graphical data are the mean ± SEM. $p < 0.05$: *vs. pre-MI, †vs. pre-Tx, ‡vs. PBS, §vs. oEPC, $^{\|}$vs. yEPC, $^{\#}$vs. yEPC + siTERT, Student's *t*-test (pre-MI, pre-Tx, $n =$ 20 per group. At 30 days post-Tx, PBS, $n = 10$; oEPC, $n = 11$; yEPC, $n = 17$; yEPC + si*TERT*, $n = 10$; yEPC + siGDF11, $n = 11$). **e**, **f** Quantitative analysis of LV weights (**e**) and infarct size (**f**) in the MI hearts receiving young CD133$^+$/VEGFR2$^+$ cells alone or plus siTERT or siGDF11 at day 30 post-Tx. yEPC-treated MI hearts had significant decrease in LV weight and infarct size, and siTERT or siGDF11 canceled this decrease. All graphical data are the mean ± SEM. $p < 0.05$: ‡vs. PBS, §vs. oEPC, $^{\|}$vs. yEPC, Student's *t*-test (PBS, $n = 5$; old EPC, $n = 6$; young EPC, $n = 12$; young EPC + si*TERT*, $n = 5$; young EPC + siGDF11, $n = 6$)

Discussion

This study identifies TERT-mediated control of GDF11-based rejuvenation of senescent VEGFR2$^+$/CD133$^+$ cells as a TERT-dependent actionable target with potential relevance for the treatment of MI in the elderly. GDF11 has recently emerged as a powerful anti-aging candidate, found in young blood, capable of rejuvenating a number of aged tissues, such as heart, skeletal muscle, and brain. However, some evidences showed that elevating blood levels of GDF11 in the aged might cause more harm than good [35], and GDF11 administration does not extend lifespan in a mouse model of premature aging [36]. In the present study, under hypoxic conditions, only the overexpression of TERT in old VEGFR2$^+$/CD133$^+$ cells significantly decreased senescence and apoptosis, increased proliferation, and

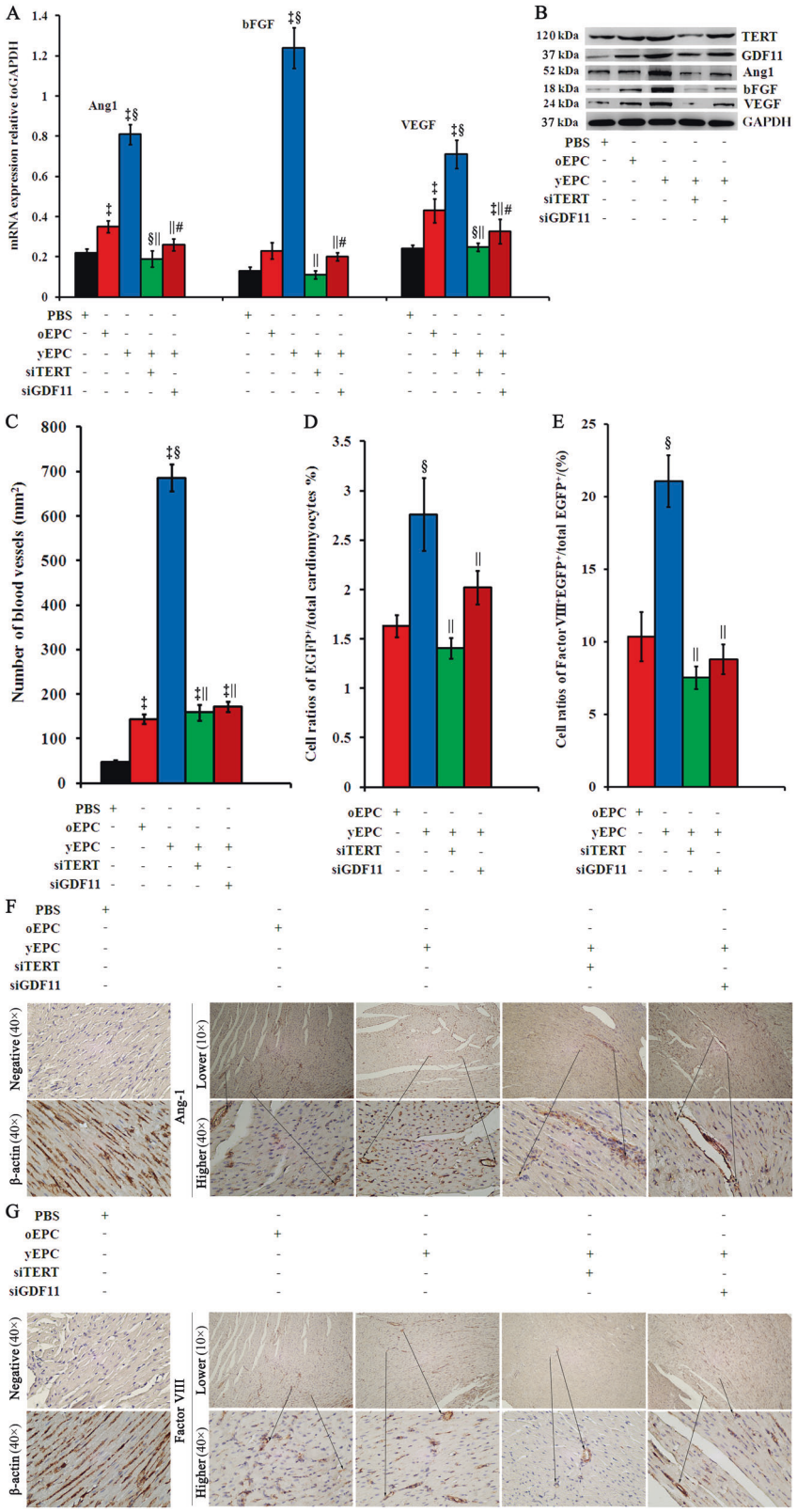

Fig. 10 (Continued)

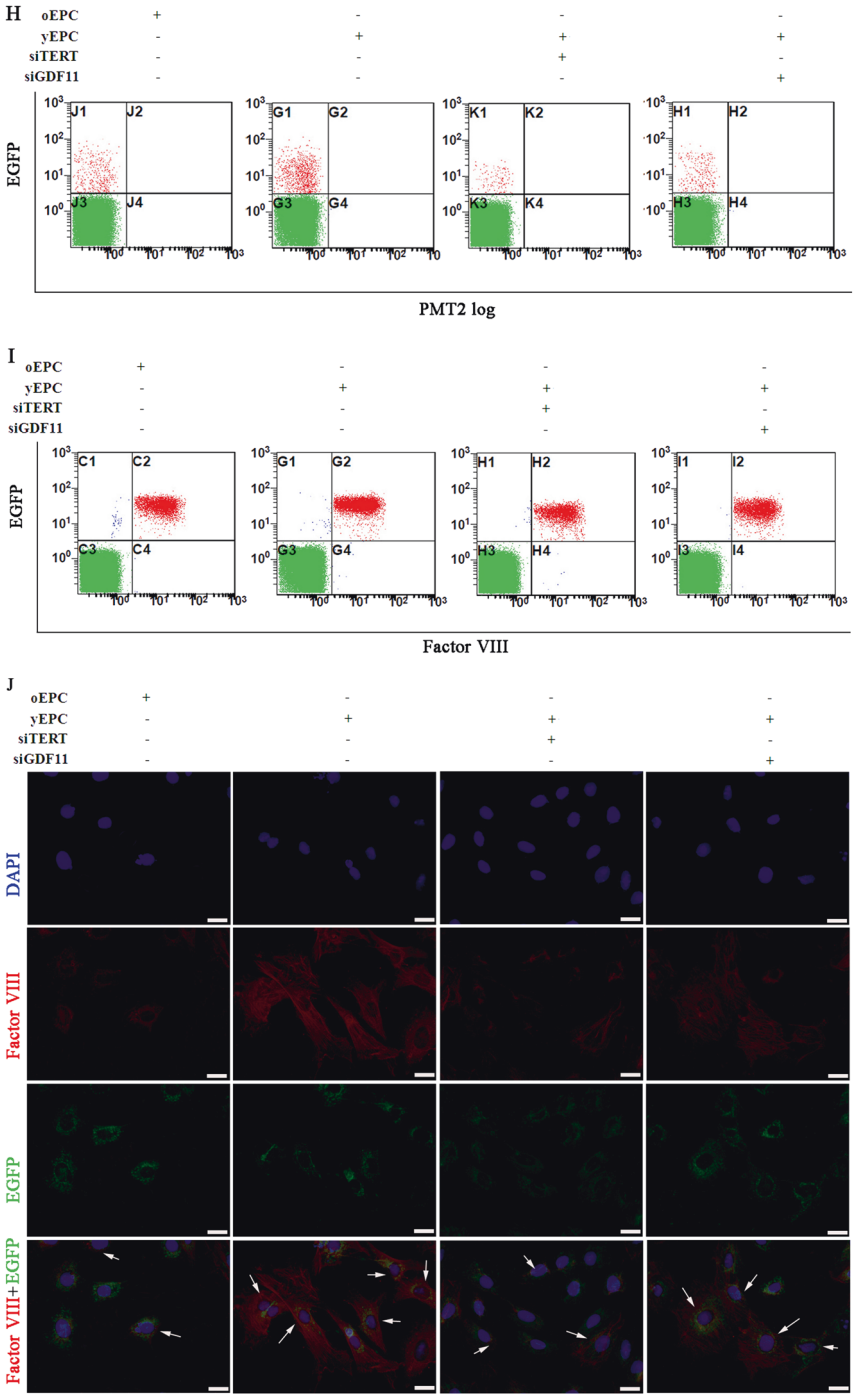

Fig. 10 (Continued)

produced the pronounced effects of GDF11-mediated rejuvenation. These data suggest maintaining high expression of TERT is a necessary to prevent senescence of old VEGFR2^{+}/CD133^{+} cells, and any effect of extrinsic GDF11 rejuvenation must be combined with adequate levels of intrinsic TERT protein. This may explain why GDF11 administration did not serve as a rejuvenator of aged skeletal muscle satellite cells in a previous study [37]. This supports the current controversy surrounding GDF11, as GDF11 can act either as a rejuvenating factor or a futile protein depending on the level of endogenous TERT expression.

EPC senescence was associated with a reduction of numbers and impairment of activity in the EPCs [38]. However, few have evaluated the senescence of EPCs in post-infarction HF with older age. In our study, the finding

Fig. 10 Depletion of GDF11 or TERT impaired angiogenesis and vascular function of young $CD133^+/VEGFR2^+$ cells in vivo. **a** mRNA expression of Ang-1, bFGF, and VEGF in old MI hearts treated with PBS, old $CD133^+/VEGFR2^+$ cells, young $CD133^+/VEGFR2^+$ cells in the presence/absence of siTERT/siGDF11 evaluating by real-time RT-PCR. **b** Western blot showed that young $CD133^+/VEGFR2^+$ cells therapy upregulated protein expression of TERT, GDF11, Ang-1, bFGF, and VEGF compared with PBS injection or old $CD133^+/VEGFR2^+$ cells therapy, whereas siGDF11 significantly reduced their expression, and siTERT further abolished theses expression. **c** Reduction of siTERT or siGDF11 in angiogenesis induced by yEPC therapy in old MI hearts was determined by the number of factor VIII positive-staining vessels per mm^2 under high-power field view by immunohistochemistry. **d**, **e** FACS assessment of the percentages of EGFP-positive cells ($EGFP^+$) relative to the whole ventricular cell population (**d**) and factor VIII (angiogenesis marker), and EGFP double-positive cells (factor $VIII^+EGFP^+$) relative to the whole $EGFP^+$ population (**e**). All graphical data are the mean ± sEM. $^{\ddagger}p < 0.05$ vs. PBS, $^{\S}p < 0.05$ vs. oEPC, $^{\|}p < 0.05$ vs. yEPC, $^{\#}p < 0.05$ vs. yEPC + siTERT, Student's *t*-test ($n = 5$ per group). **f**, **g** Representative images of Ang-1 (brown, **f**) or factor VIII (brown, **g**) under lower magnification (×10, upper) and higher magnification (×40, lower) by staining cardiomyocytes and vessels in the infarct and peri-infarct area from old MI hearts treated with old $CD133^+/VEGFR2^+$ cells, young $CD133^+/VEGFR2^+$ cells in the presence/absence of siTERT/siGDF11. Staining with anti-β-actin antibody or without primary antibody in the MI hearts treated with PBS served as a positive control and negative control (×40). Arrows indicated the origination of the higher magnification images from the region of interesting in the lower magnification images. **h**, **i** Representative phenotypes of gated $EGFP^+$ (**h**) and factor $VIII^+EGFP^+$ (**i**) cells evaluated by FACS in transplanted $CD133^+/VEGFR2^+$ cells. Although the survival and angiogenesis degree of young $CD133^+/VEGFR2^+$ cells were significantly greater than those of old cells, significantly decreased young cell survival and angiogenesis was seen in young cells pre-treated with siTERT or siGDF11. **j** Immunofluorescence staining showing that transplanted cells expressed factor VIII. The transplanted cells were prelabeled with EGFP (green); the nuclei were stained with DAPI (blue), and the EC cytoplasm was stained with anti-factor VIII antibody (red). Engrafted EGFP-prelabeled cells expressing factor VIII were the most numerous in yEPC MI hearts, and were lowest in siTERT-transfected young $CD133^+/VEGFR2^+$ cells (arrows). Scale bars = 50 μm

of a reduced number of EPCs isolated from circulating blood with increasing age was in line with increased senescence. Moreover, our study revealed that after culture in vitro, senescent $VEGFR2^+/CD133^+$ cells (late-outgrowth EPCs) from old patients had poorer survival, decreased colony forming and migratory capacity, and impaired incorporation into tube-like structures. However, in vitro exposure of old $VEGFR2^+/CD133^+$ cells to adTERT produced significant increases in telomerase activity, cell proliferation and differentiation. GDF11 alone did not rejuvenate senescent $VEGFR2^+/CD133^+$ cells; this occurred with the participation of TERT. Taken together, our data indicated that TERT could act on old $VEGFR2^+/CD133^+$ cells to alter GDF11 rejuvenation function.

Understanding how TERT controls GDF11 activity is essential to move the field forward and help develop clinical studies to evaluate the efficacy of GDF11-mediated rejuvenation in old EPCs. How age affects the survival of EPCs is complex, and involves alterations in the expression of multiple imprinted growth-regulatory genes on cell senescence, including telomere shortening and dysfunction [38], eNOS downregulation [39], decreased circulating proangiogenic factors [40], and perhaps decreased GDF11 [4]. We investigated the molecular mechanism behind the survival of $VEGFR2^+/CD133^+$ cells in old-age patients with AMI. Compared with $VEGFR2^+/CD133^+$ cells from young patients, there was a lower expression of TERT, GDF11, eNOS, Ang-1, bFGF, and VEGF in $VEGFR2^+/CD133^+$ cells from old patients after AMI. GDF11 exerts its function by inducing canonical Smads signaling pathway [41]. This study showed that the exogenous supplement of rhGDF11 amplified itself at the total mRNA and protein levels in the old EPCs and increased its downstream effector Smad2/3 phosphorylation and nuclear translocation, which was prevented by adding its antagonist, consisting of data from the oligodendrocyte precursor cells by Shi et al., showing that addition of rhGDF11 downregulated the expression of its downstream effector Pax6 in the precursor cells from $GDF11^{-/-}$ mouse embryos [42]. Consistent with this, Oh et al. also observed that both intrinsic GDF11 and exogenous GDF11 tagged with a Flag epitope at the N terminus of the mature region were able to induce Smad2 phosphorylation in Xenopus ectodermal explants [43]. These data suggested that the rhGDF11 used in their study exhibits equivalent activity from a signaling and antagonist perspective as intrinsic GDF11. However, addition of rhGDF11 alone did not significantly increase their expression of TERT, ultimately causing no significant extension of cell lifespan of the old $VEGFR2^+/CD133^+$ cells when compared with addition of adTERT. Only rhGDF11 combined with adTERT transfection could cause a significant extension of cell lifespan in the old $VEGFR2^+/CD133^+$ cells by activating phosphorylation of Smad2/3 in old $VEGFR2^+/CD133^+$ cells, and consequently induced less apoptosis by upregulation of anti-apoptotic protein Bcl2 and downregulation of apoptotic protein caspase 3. These anti-apoptotic effects could be attenuated by the Smad2/3 inhibitor SB431542. Taken together, the data indicated that exogenous rhGDF11 in combination with adTERT transfection could improve survival of older $VEGFR2^+/CD133^+$ cells under hypoxic injury, possibly through the canonical (Smad2/3) signaling pathway. In addition, GDF11 activation results in activation of several other non-Smad signaling pathways and regulates expression of its target nuclear genes [44], involving the ERK1/2, JNK, Akt, and the eNOS pathway [45]. This study showed that the interaction between GDF11 and TERT in rejuvenating old EPCs is consistent with increasing the phosphorylation of eNOS and consequently increased NO production and NOS activity in old EPCs. Consistent with the eNOS increase,

TERT promoted GDF11-mediated rejuvenation, secretion, vessel formation, vessel length, branch formation, and neovascularization of old VEGFR2$^+$/CD133$^+$ cells, whereas depletion of TERT attenuates these effects. Our results are similar to the senescence of outgrowth endothelial cells, which have limited regenerative potential and impaired vasoreparative properties, due to lowered telomerase activity and shortened telomeres [46]. Moreover, upregulation of cardiac telomere-stabilizing proteins through long- and short-term voluntary physical exercise can induce antisenescent and protective effects by increasing the expression of TERT and eNOS [47]. Thus, there is a possible direct link between the senescence of old VEGFR2$^+$/CD133$^+$ cells, decrease of TERT expression, and lowered eNOS activity associated with aging, indicating that TERT is a powerful transcription factor for GDF11-mediated promotion of rejuvenation of vascular reactivity and angiogenesis of old VEGFR2$^+$/CD133$^+$ cells. This study further showed that treatment with a specific inhibitor of eNOS, such as L-NAME, significantly attenuated the effects of GDF11 and TERT on secretion of proangiogenic factors, such as Ang-1, bFGF, and VEGF. eNOS phosphorylation contributes to Ang-1-dependent inhibition of VEGF-induced endothelial permeability in vitro [48]. The eNOS-mediated improvement of secretion of proangiogenic factors of old VEGFR2$^+$/CD133$^+$ cells can partially explain the protective and angiogenic effects of adTERT and rhGDF11. Taken together, the data indicated that sufficient TERT is necessary to activate GDF11-mediated rejuvenation of senescent VEGFR2$^+$/CD133$^+$ cells through the canonical (Smad2/3) and noncanonical (eNOS) signaling pathways, providing evidence that pharmacological increase of TERT enhances the GDF11-mediated rejuvenation pathway in vitro.

This rejuvenation effect of TERT on GDF11 has conversely been confirmed by depletion of TERT and GDF11 inducing senescence of young VEGFR2$^+$/CD133$^+$ cells. In this study, knockdown of GDF11 or TERT caused significant changes in GDF11-mediated signaling antibody array, including inhibiting GDF11 expression, increasing the expression of aging factors, p21 and p27, attenuating the expression of the Smad2/3 and eNOS signaling pathways, such as Smad2/3, Bcl2, eNOS, Ang-1, bFGF, and VEGF, which caused significant worsening of apoptosis, resulting in decreased proliferation, angiogenesis, neovascularization, and senescence. In comparison, depletion of TERT caused further increase of the expression of senescence markers, p21 and p16, than depletion of GDF11, which in turn confirmed TERT control of GDF11-mediated rejuvenation of VEGFR2$^+$/CD133$^+$ cells.

It is now clear that the nucleocytoplasmic distributions of Smads, in the absence and the presence of a TGFβ-superfamily signal, are not static; the Smads are continuously shuttling between the nucleus and the cytoplasm in both conditions [49]. In this study, we found that rhGDF11 combined with adTERT promotes Smad2/3 export from the nucleus to cytosol. Nucleocytoplasmic shuttling in the epidermis of the skin is essential for tissue development, homeostasis, and repair [50]. Smad3 preferentially localizes within the nucleus, and exerts a neural lineage promoting role during ESCs differentiation. In contrast to Smad3, Smad2 resides in the cytoplasm, and is essential for proper epiblast and germ layer differentiation from ESCs [51]. In our study, GDF11 cooperated with TERT to promote survival and angiogenesis of old VEGFR2$^+$/CD133$^+$ cells in synchronization with Smad2/3 nucleocytoplasmic shuttling, suggesting that nucleocytoplasmic shuttling of Smads enables old VEGFR2$^+$/CD133$^+$ cells to activate antiapototic signal and provides the flexibility of GDF11-mediated rejuvenation. It should be noted, however, that in this study, it is not clear how GDF11 mediates nuclear import and export of all components in Smads.

Recent findings show reduced telomerase activity and decreased expression of several telomerase genes results in premature aging of hematopoietic stem cells at a young age [52]. Depletion of TERT or GDF11 was implicated in inhibition of myocardial repair induced by young VEGFR2$^+$/CD133$^+$ cells. After transplantation into ischemic hearts, GDF11 expression were significantly lower in the infarcted hearts receiving siGDF11-treated young VEGFR2$^+$/CD133$^+$ cell therapy than in those receiving young VEGFR2$^+$/CD133$^+$ cells injection alone, and siTERT further enhanced this decrease. These differences were consistently associated with deterioration in cardiac function and left-ventricular structural remodeling of hearts treated with siTERT or siGDF11-treated young cells after MI. Compared with old VEGFR2$^+$/CD133$^+$ cells therapy or PBS injection, simple transplantation of young VEGFR2$^+$/CD133$^+$ cells caused higher expression of GDF11 and TERT, leading to beneficial effects, including improving HF and cardiac remodeling, and reducing infarct size. Thus, the benefit of cell transplantation appears to be inextricably linked with the extent of GDF11 and TERT coactivation, suggesting that GDF11 and telomere is involved in aging and the development of age-related heart dysfunction [53].

On the other hand, depletion of GDF11 or TERT downregulated target signaling, including Smad2/3 and eNOS signaling pathways. The downregulation of these signal molecules induced by GDF11 or TERT knockdown was associated with a significant decrease of the ratio of young VEGFR2$^+$/CD133$^+$ cells cultured in vitro differentiating into blood vascular endothelial cells (vasculogenesis) or young VEGFR2$^+$/CD133$^+$ cells engrafted into the infarcted hearts developing new blood vessels (angiogenesis). These data demonstrate that depletion of GDF11

or TERT both reduced the expression of endogenous vascular permeabilizing factors, including Ang-1, bFGF, and VEGF, which are the target genes of eNOS-mediated angiogenesis under ischemic conditions [54, 55]. The interaction between GDF11 and TERT in regulating Smad2/3-mediated anti-apoptotic and pro-apoptotic proteins was consistent with altered survival and apoptosis of young $VEGFR2^+/CD133^+$ cells after GDF11 or TERT knockdown, or control siRNA addition. Our results are similar to that of the study of Xu et al. [56] wherein cell proliferation and apoptosis were dependent on phosphorylation levels of smad2/3, the expression of caspase 3, and the ratio of Bcl2 to Bax.

In summary, the identification of TERT as a GDF11-dependent regulator of rejuvenation old $VEGFR2^+/CD133^+$ cells from the older MI patients or senescence of young $VEGFR2^+/CD133^+$ cells from the younger MI patients opens new perspectives for the molecular mechanism of GDF11-mediated cellular rejuvenation. TERT modulation of GDF11 might be exploited therapeutically to enhance rejuvenation of senescent stem cells in the myocardial ischemic microenvironment, and the availability of drugs that target the TERT-mediated GDF11 signaling pathway warrants future studies aimed at the clinical translation of GDF11-mediated rejuvenation enhancement in senile degenerative artery disease.

Acknowledgements This work was supported by grants from the National Natural Sciences Foundation of China (81270172, to SZ), Guangdong Provincial Natural Science Fund (1814050000493, to SZ), and the Shanghai Nature Science Fund (16ZR1432700, to LZ).

Compliance with ethical standards

Conflict of interest The authors declare that they have no conflict of interest.

References

1. Camici GG, Savarese G, Akhmedov A, Lüscher TF. Molecular mechanism of endothelial and vascular aging: implications for cardiovascular disease. Eur Heart J. 2015;36:3392–403.
2. Yepuri G, Sukhovershin R, Nazari-Shafti TZ, Petrascheck M, Ghebre YT, Cooke JP. Proton pump inhibitors accelerate endothelial senescence. Circ Res. 2016;118:e36–42.
3. Aragona CO, Imbalzano E, Mamone F, Cairo V, Lo Gullo A, D'Ascola A, et al. Endothelial progenitor cells for diagnosis and prognosis in cardiovascular disease. Stem Cells Int. 2016;2016:8043792.
4. Onodera K, Sugiura H, Yamada M, Koarai A, Fujino N, Yanagisawa S, et al. Decrease in an anti-aging factor, growth differentiation factor 11, in chronic obstructive pulmonary disease. Thorax. 2017;72:893–904.
5. Katsimpardi L, Litterman NK, Schein PA, Miller CM, Loffredo FS, Wojtkiewicz GR, et al. Vascular and neurogenic rejuvenation of the aging mouse brain by young systemic factors. Science. 2014;344:630–4.
6. Rodgers BD. The immateriality of circulating GDF11. Circ Res. 2016;118:1472–4.
7. Walker RG, Poggioli T, Katsimpardi L, Buchanan SM, Oh J, Wattrus S, et al. Biochemistry and biology of GDF11 and myostatin: similarities, differences and questions for future investigation. Circ Res. 2016;118:1125–42.
8. Xiong S, Patrushev N, Forouzandeh F, Hilenski L, Alexander RW. PGC-1α modulates telomere function and DNA damage in protecting against aging-related chronic diseases. Cell Rep. 2015;12:1391–9.
9. Madonna R, Taylor DA, Geng YJ, De Caterina R, Shelat H, Perin EC, et al. Transplantation of mesenchymal cells rejuvenated by the overexpression of telomerase and myocardin promotes revascularization and tissue repair in a murine model of hindlimb ischemia. Circ Res. 2013;113:902–14.
10. Cho HJ, Lee N, Lee JY, Choi YJ, Ii M, Wecker A, et al. Role of host tissues for sustained humoral effects after endothelial progenitor cell transplantation into the ischemic heart. J Exp Med. 2007;204:3257–69.
11. Zhang S, Zhao L, Shen L, Xu D, Huang B, Wang Q, et al. Comparison of various niches for endothelial progenitor cell therapy on ischemic myocardial repair: coexistence of host collateralization and Akt-mediated angiogenesis produces a superior microenvironment. Arterioscler Thromb VascBiol. 2012;32:910–23.
12. Zhang S, Zhao L, Wang J, Chen N, Yan J, Pan X. HIF-2α and Oct4 have synergistic effects on survival and myocardial repair of very small embryonic-like mesenchymal stem cells in infarcted hearts. Cell Death Dis. 2017;8:e2548.
13. Wang JH, Zhao L, Pan X, Chen NN, Chen J, Gong QL, et al. Hypoxia-stimulated cardiac fibroblast production of IL-6 promotes myocardial fibrosis via the TGF-β1 signaling pathway. Lab Invest. 2016;96:839–52.
14. Muroya Y, He X, Fan L, Wang S, Xu R, Fan F, et al. Enhanced renal ischemia-reperfusion injury in aging and diabetes. Am J Physiol Renal Physiol. 2018. 10.1152/ajprenal.00184.2018.
15. Jodon de Villeroché V, Avouac J, Ponceau A, Ruiz B, Kahan A, Boileau C, et al. Enhanced late-outgrowth circulating endothelial progenitor cell levels in rheumatoid arthritis and correlation with disease activity. Arthritis Res Ther. 2010;12:R27.
16. Ahmed FW, Rider R, Glanville M, Narayanan K, Razvi S, Weaver JU. Metformin improves circulating endothelial cells and endothelialprogenitor cells in type 1 diabetes: MERIT study. Cardiovasc Diabetol. 2016;15:116.
17. Morishita T, Uzui H, Ikeda H, Amaya N, Kaseno K, Ishida K, et al. Association of CD34/CD133/VEGFR2-positive cell numbers with eicosapentaenoic acid and postprandial hyperglycemia in patients with coronary artery disease. Int J Cardiol. 2016;221:1039–42.
18. Fortunato O, Spinetti G, Specchia C, Cangiano E, Valgimigli M, Madeddu P. Migratory activity of circulating progenitor cells and serum SDF-1α predict adverse events in patients with myocardial infarction. Cardiovasc Res. 2013;100:192–200.
19. de la Puente P, Muz B, Azab F, Azab AK. Cell trafficking of endothelial progenitor cells in tumor progression. Clin Cancer Res. 2013;19:3360–8.
20. Chang WY, Lavoie JR, Kwon SY, Chen Z, Manias JL, Behbahani J, et al. Feeder-independent derivation of induced-pluripotent stem cells from peripheral blood endothelial progenitor cells. Stem Cell Res. 2013;10:195–202.

21. Yu M, Liu Q, Sun J, Yi K, Wu L, Tan X. Nicotine improves the functional activity of late endothelial progenitor cells via nicotinicacetylcholine receptors. Biochem Cell Biol. 2011;89:405–10.
22. Miyauchi H, Minamino T, Tateno K, Kunieda T, Toko H, Komuro I. Akt negatively regulates the in vitro lifespan of human endothelial cells via a p53/p21-dependent pathway. EMBO J. 2004;23:212–20.
23. Paschalaki KE, Starke RD, Hu Y, Mercado N, Margariti A, Gorgoulis VG, et al. Dysfunction of endothelial progenitor cells from smokers and chronic obstructive pulmonary disease patients due to increased DNA damage and senescence. Stem Cells. 2013;31:2813–26.
24. Patel J, Donovan P, Khosrotehrani K. Concise review: functional definition of endothelial progenitor cells: a molecular perspective. Stem Cells Transl Med. 2016;5:1302–6.
25. Dashnyam K, Jin GZ, Kim JH, Perez R, Jang JH, Kim HW. Promoting angiogenesis with mesoporous microcarriers through a synergistic action of delivered silicon ion and VEGF. Biomaterials. 2017;116:145–57.
26. Blau HM, Cosgrove BD, Ho AT. The central role of muscle stem cells in regenerative failure with aging. Nat Med. 2015;21:854–62.
27. Egerman MA, Cadena SM, Gilbert JA, Meyer A, Nelson HN, Swalley SE, et al. GDF11 increases with age and inhibits skeletal muscle regeneration. Cell Metab. 2015;22:164–74.
28. Heiss EH, Dirsch VM. Regulation of eNOS enzyme activity by posttranslational modification. Curr Pharm Des. 2014;20:3503–13.
29. Zhang J, Li Y, Li H, Zhu B, Wang L, Guo B, et al. GDF11 improves angiogenic function of EPCs in diabetic limb ischemia. Diabetes. 2018;67:2084–95.
30. Finkenzeller G, Stark GB, Strassburg S. Growth differentiation factor 11 supports migration and sprouting of endothelial progenitor cells. J Surg Res. 2015;198:50–6.
31. Fu M, Li Z, Tan T, Guo W, Xie N, Liu Q, et al. Akt/eNOS signaling pathway mediates inhibition of endothelial progenitor cells by palmitate-induced ceramide. Am J Physiol Heart Circ Physiol. 2015;308:H11–7.
32. Atluri P, Trubelja A, Fairman AS, Hsiao P, MacArthur JW, Cohen JE, et al. Normalization of postinfarct biomechanics using a novel tissue-engineered angiogenic construct. Circulation. 2013;128 (11Suppl 1):S95–104.
33. Hermansen SE, Lund T, Kalstad T, Ytrehus K, Myrmel T. Adrenomedullin augments the angiogenic potential of late outgrowth endothelial progenitorcells. Am J Physiol Cell Physiol. 2011;300:C783–791.
34. Nguyen PK, Rhee JW, Wu JC. Adult stem cell therapy and heart failure, 2000 to 2016: a systematic review. JAMA Cardiol. 2016;1:831–41.
35. Harper SC, Brack A, MacDonnell S, Franti M, Olwin BB, Bailey BA, et al. Is growth differentiation factor 11 a realistic therapeutic for aging-dependent muscle defects? Circ Res. 2016;118: 1143–50.
36. Freitas-Rodríguez S, Rodríguez F, Folgueras AR. GDF11 administration does not extend lifespan in a mouse model of premature aging. Oncotarget. 2016;7:55951–6.
37. Hinken AC, Powers JM, Luo G, Holt JA, Billin AN, Russell AJ. Lack of evidence for GDF11 as a rejuvenator of aged skeletal muscle satellite cells. Aging Cell. 2016;15:582–4.
38. Nollet E, Hoymans VY, Rodrigus IR, De Bock D, Dom M, Van Hoof VOM, et al. Accelerated cellular senescence as underlying mechanism for functionally impaired bone marrow-derived progenitor cells in ischemic heart disease. Atherosclerosis. 2017; 260:138–46.
39. Guo Y, Li P, Gao L, Zhang J, Yang Z, Bledsoe G, et al. Kallistatin reduces vascular senescence and aging by regulating microRNA-34a-SIRT1 pathway. Aging Cell. 2017;16:837–46.
40. Ali M, Mehmood A, Anjum MS, Tarrar MN, Khan SN, Riazuddin S. Diazoxide preconditioning of endothelial progenitor cells from streptozotocin-induced type 1 diabetic rats improves their ability to repair diabetic cardiomyopathy. Mol Cell Biochem. 2015;410:267–79.
41. Mei W, Xiang G, Li Y, Li H, Xiang L, Lu J, et al. GDF11 protects against endothelial injury and reduces atherosclerotic lesion formation in apolipoprotein E-null mice. Mol Ther. 2016;24:1926–38.
42. Shi Y, Liu J. Gdf11 facilitates temporal progression of neurogenesis in the developing spinal cord. J Neurosci. 2011;31: 883–93.
43. Oh SP, Yeo CY, Lee Y, Schrewe H, Whitman M, Li E. Activin type IIA and IIB receptors mediate Gdf11 signaling in axial vertebral patterning. Genes Dev. 2002;16:2749–54.
44. Zhang Y, Wei Y, Liu D, Liu F, Li X, Pan L, et al. Role of growth differentiation factor 11 in development, physiology and disease. Oncotarget. 2017;8:81604–16.
45. Bos D, van der Rijk MJ, Geeraedts TE, Hofman A, Krestin GP, Witteman JC, et al. Intracranial carotid artery atherosclerosis: prevalence and risk factors in the general population. Stroke. 2012;43:1878–84.
46. Medina RJ, O'Neill CL, O'Doherty TM, Chambers SE, Guduric-Fuchs J, Neisen J, et al. Ex vivo expansion of human outgrowth endothelial cells leads to IL-8-mediated replicative senescence and impaired vasoreparative function. Stem Cells. 2013;31:1657–68.
47. Werner C, Hanhoun M, Widmann T, Kazakov A, Semenov A, Pöss J, et al. Effects of physical exercise on myocardial telomere-regulating proteins, survival pathways, and apoptosis. J Am Coll Cardiol. 2008;52:470–82.
48. Oubaha M, Gratton JP. Phosphorylation of endothelial nitric oxide synthase by atypical PKC zeta contributes to angiopoietin-1-dependent inhibition of VEGF-induced endothelial permeability in vitro. Blood. 2009;114:3343–51.
49. Hill CS. Nucleocytoplasmic shuttling of Smad proteins. Cell Res. 2009;19:36–19.
50. Sharili AS, Connelly JT. Nucleocytoplasmic shuttling: a common theme in mechanotransduction. Biochem Soc Trans. 2014;42:645–549.
51. Liu L, Liu X, Ren X, Tian Y, Chen Z, Xu X, et al. Smad2 and Smad3 have differential sensitivity in relaying TGFβ signaling and inversely regulateearly lineage specification. Sci Rep. 2016;6:21602.
52. Schafer MJ, Atkinson EJ, Vanderboom PM, Kotajarvi B, White TA, Moore MM, et al. Quantification of GDF11 and myostatin in human aging and cardiovascular disease. Cell Metab. 2016;23:1207–15.
53. Camici GG, Savarese G, Akhmedov A, Lüscher TF. Molecular mechanism of endothelial and vascular aging: implications for cardiovascular disease. Eur Heart J. 2015;36:3392–403.
54. Matsumura M, Fukuda N, Kobayashi N, Umezawa H, Takasaka A, Matsumoto T, et al. Effects of atorvastatin on angiogenesis in hindlimb ischemia and endothelial progenitor cell formation in rats. J Atheroscler Thromb. 2009;16:319–26.
55. Hanawa K, Ito K, Aizawa K, Shindo T, Nishimiya K, Hasebe Y, et al. Low-intensity pulsed ultrasound induces angiogenesis and ameliorates left ventricular dysfunction in a porcine model of chronic myocardial ischemia. PLoS ONE. 2014;9:e104863.
56. Xu P, Zhang Y, Liu Y, Yuan Q, Song L, Liu M, et al. Fibroblast growth factor 21 attenuates hepatic fibrogenesis through TGF-β/smad2/3 and NF-κB signaling pathways. Toxicol Appl Pharmacol. 2016;290:43–53.